Semiparametric inference on the fractal index of Gaussian and conditionally Gaussian time series data

Mikkel Bennedsen

CREATES Research Paper 2016-21

Department of Economics and Business Economics
Aarhus University
Fuglesangs Allé 4
DK-8210 Aarhus V
Denmark

Email: oekonomi@au.dk
Tel: +45 8716 5515

Semiparametric inference on the fractal index of Gaussian and conditionally Gaussian time series data*

Mikkel Bennedsen†

August 4, 2016

Abstract

Using theory on (conditionally) Gaussian processes with stationary increments developed in Barndorff-Nielsen et al. (2009, 2011), this paper presents a general semiparametric approach to conducting inference on the fractal index, α, of a time series. Our setup encompasses a large class of Gaussian processes and we show how to extend it to a large class of non-Gaussian models as well. It is proved that the asymptotic distribution of the estimator of α does not depend on the specifics of the data generating process for the observations, but only on the value of α and a "heteroskedasticity" factor. Using this, we propose a simulation-based approach to inference, which is easily implemented and is valid more generally than asymptotic analysis. We detail how the methods can be applied to test whether a stochastic process is a non-semimartingale. Finally, the methods are illustrated in two empirical applications motivated from finance. We study time series of log-prices and log-volatility from 29 individual US stocks; no evidence of non-semimartingality in asset prices is found, but we do find evidence of non-semimartingality in volatility. This confirms a recently proposed conjecture that stochastic volatility processes of financial assets are *rough* (Gatheral et al., 2014).

Keywords: Fractal index; Monte Carlo simulation; roughness; semimartingality; fractional Brownian motion; stochastic volatility.

JEL Classification: C12, C22, C63, G12

MSC 2010 Classification: 60G10, 60G15, 60G17, 60G22, 62M07, 62M09, 65C05

---

*I would like to thank Professor Asger Lunde and Dr. Mikko S. Pakkanen for insightful discussions relating to fractal processes and Solveig Sørensen for competent and precise proof reading of the manuscript. The research has been supported by CREATES (DNRF78), funded by the Danish National Research Foundation, by Aarhus University Research Foundation (project "Stochastic and Econometric Analysis of Commodity Markets"), and by Aage and Ylva Nimbs Foundation.

†Department of Economics and Business Economics and CREATES, Aarhus University, Fuglesangs Allé 4, 8210 Aarhus V, Denmark. E-mail: mbennedsen@econ.au.dk

1 Introduction

This paper is concerned with conducting statistical inference on the so-called *fractal index* of a time series. Formally, we consider (conditionally) Gaussian stochastic processes X, with stationary increments satisfying

$$\mathbb{E}[|X_{t+h} - X_t|^p] \sim C_p |h|^{(2\alpha+1)p/2}, \quad h \downarrow 0, \tag{1.1}$$

for $p > 0$, $C_p > 0$, and $\alpha \in \left(-\frac{1}{2}, \frac{1}{2}\right)$. The parameter α is termed the fractal index because it, under mild assumptions, is related to the *fractal dimension* $D = \frac{3}{2} - \alpha$ of the sample paths of the process X (Falconer, 1990; Gneiting et al., 2012). The parameter α is also called the *roughness parameter* as it reflects itself in the pathwise properties of X, as will be made precise in Proposition 2.1 below. Informally, $\alpha < 0$ implies rough sample paths of X, while $\alpha > 0$ implies smooth sample paths of the process. After a log-transformation, the scaling relationship (1.1) suggests a straightforward estimation procedure of α based on OLS regression. As we shall see, the OLS estimator, $\hat{\alpha}$, of α comes with a central limit theorem (CLT) of the type

$$\tau_n \left(\hat{\alpha} - \alpha\right) \xrightarrow{d} Z_p \cdot S_p, \quad n \to \infty, \tag{1.2}$$

where n is the number of observations, τ_n is a rate sequence (e.g. $\tau_n = \sqrt{n}$), and Z_p is a random variable. $S_p > 0$ is a heteroscedasticity factor, which is equal to one when X is Gaussian and different from one otherwise. It is well known that the random variable Z_p is Gaussian when $\alpha \in (-1/2, 1/4]$ (e.g. Breuer and Major, 1983). However, when $\alpha > 1/4$, Taqqu (1975) showed that the distribution of Z_p is given by the *Rosenblatt distribution* in a quite complicated way. What is more, although the distribution of Z_p is known in theory, it is generally infeasible to calculate it explicitly when $p \neq 2$.

The contribution of this paper is to suggest bootstrap/Monte Carlo procedures to the problem of testing statistical hypotheses regarding the fractal index, as well as computing confidence intervals around the estimated value. Specifically, we prove that (1.2) holds for a large class of fractal processes, where the distribution of the random variable Z_p is invariant to the actual data generating process (DGP) of X. That is, the distribution of Z_p depends only on the value of α, i.e. of the roughness properties of the data. We suggest a simple estimator of S_p and then to approximate the distribution of Z_p by Monte Carlo simulation. The key to the Monte Carlo approach is the invariance of the distribution of Z_p, enabling one to approximate it by any (Gaussian) fractal process; the obvious choice for such an *auxiliary process* is the canonical fractal process, the fractional Brownian motion (fBm, Mandelbrot and Van Ness, 1968). The upshot is that the methods presented in this paper are valid for all $p > 0$ and $\alpha \in (-1/2, 1/2)$. Indeed, since the auxiliary simulations directly approximate the distribution of Z_p, it is not necessary to distinguish between the Gaussian case ($\alpha \leq 1/4$) and the Rosenblatt case ($\alpha > 1/4$), nor of taking into account the actual convergence rate, τ_n.

Another advantage of the simulation-based approach, as compared to asymptotic analysis, is that the OLS estimator of α requires a choice of bandwidth $m \in \mathbb{N}$, denoting the number of data points used in the regression. The distribution of Z_p will in turn depend on this parameter and this distribution gets increasingly complicated with increasing m. Our approach trivially allows for any $m \geq 2$ and we will exploit this to give some guidelines on how to select m. In summary, simulations show that choosing m slightly larger than 2 results in a good trade-off between small bias (obtained by having m small) and low variance (obtained by larger m). We recommend setting $m = 3$ and will do so in our applications. This is slightly at odds with conventional wisdom which recommends $m = 2$ (e.g. Davies and Hall, 1999).

Most previous work on inference for the fractal index has been done assuming Gaussianity of X; notable exceptions being Chan and Wood (2004) and Achard and Coeurjolly (2010). Indeed, in a survey of the asymptotic theory, Gneiting et al. (2012) section 3.1., reports that "a general non-Gaussian theory remains lacking". Below, we will show how to extend the theory to a large class of non-Gaussian processes obtained by *volatility modulation* of an otherwise Gaussian process. When X is a so-called volatility modulated Brownian semistationary process (Barndorff-Nielsen and Schmiegel, 2007, 2009) a CLT, which obeys (1.2), is derived in Theorem 4.1. When $\alpha \in (-1/2, 1/4)$, Z_p will be Gaussian with an asymptotic distribution that is feasible to calculate for $p = 2$. That is, this CLT suffers from the same drawbacks as other asymptotic approaches, as discussed above. The bootstrap approach of this paper is still valid generally, i.e. for all $\alpha \in (-1/2, 1/2)$ and $p > 0$, however.

Two different versions of the bootstrap procedure are suggested. The first method is specifically tailored to test null hypotheses such as $H_0 : \alpha = \alpha_0$ for $\alpha_0 \in (-1/2, 1/2)$; of special interest is $\alpha_0 = 0$ which means X has the same roughness as the Brownian motion and is thus, more or less, a semimartingale. For this method the auxiliary fBms are generated with fractal index α_0, i.e. the fractal index that X has under the null. The second version is tailored to make confidence intervals around the estimated value $\hat{\alpha}$: here α is first estimated from the observations of X, and then the auxiliary fBms are generated such that they have fractal index equal to $\hat{\alpha}$.

In some respects, the simulation-based approach to inference of this paper is similar to the semiparametric bootstrap method of Hall et al. (2000). Here the authors consider bootstrapping the Hurst index H of a process using the classical rescaled/range (RS) estimator of Mandelbrot and Van Ness (1968). It is well known that the fractal index of the fBm – and indeed of any *self-similar* process – is related to the Hurst index of that process through the identity $H = \alpha + \frac{1}{2}$ (e.g. Gneiting and Schlather, 2004). So, when the underlying DGP of X is self-similar (e.g. when X is an fBm), the approach of Hall et al. (2000) can be used to estimate, and make inference on, the fractal index α of X by exploiting the identity $\alpha = H - \frac{1}{2}$. However, when X is *not* self-similar, there is generally no simple relationship between H and α, and therefore RS will be inadequate to estimate α. Evidently, in this important case, the approach of Hall et al. (2000) will therefore not be applicable to perform inference on α, which is the goal in this paper. For other bootstrap approaches related to the fractal index α or the Hurst index H, see Davies and Hall (1999), Grau-Carles (2005), Kim and Nordman (2013), and Bennedsen et al. (2016).

This paper does not restrict attention to self-similar models. Indeed, most of the DGPs considered below will either be stationary or allowing α and H to vary independently of each other, or both. Time series having these features are generically not self-similar and the methods of Hall et al. (2000) do therefore not apply for such DGPs when performing inference on the fractal index for the reasons explained above. Note that especially the 'rough' case $\alpha < 0$ seems to be relevant in empirical applications. For instance, the celebrated scaling laws of Kolmogorov (Kolmogorov, 1941) predict time series of the main velocity component of turbulence with $\alpha = -1/6$, see e.g. Corcuera et al. (2013). In finance, Barndorff-Nielsen et al. (2013) and Bennedsen (2015) model electricity spot prices using fractal processes with $\alpha < 0$, and recently estimates around $\alpha \approx -0.40$ have been found for time series of volatility (Gatheral et al., 2014; Bayer et al., 2015; Bennedsen et al., 2016). Note that the DGPs underlying all these empirical examples are, besides fractal, generally believed to be stationary and therefore *not* self-similar. For this reason, an inference approach that can accomodate this – e.g. the one presented in this paper – is crucial for such applications. Additionally, the time series underlying these examples are likely non-Gaussian as well, and the present approach also allows for this, as discussed above and shown below.

The rest of the paper is structured as follows. Section 2 presents the mathematical setup and assumptions and gives an example of the kind of processes we have in mind. Section 3 presents the semiparametric estimator of the fractal index and then sets forth the two bootstrap methods. Section 4 presents some extensions to the basic setup. Section 5 contains extensive simulation evidence that the bootstrap methods work well for a wide range of DGPs, with and without the presence of stochastic volatility. Finally, Section 6 presents some empirical applications motivated from finance. Section 7 concludes. Proofs of technical results, some mathematical derivations, and details about the DGPs from the simulation study are given in the Appendix.

2 Setup

Let $(\Omega, \mathcal{F}, \mathbb{P})$ be a probability space supporting X, a one-dimensional, zero-mean, stochastic process with stationary increments. Define the *p'th order variogram* of X:

$$\gamma_p(h) := \mathbb{E}[|X_{t+h} - X_t|^p], \quad h \in \mathbb{R}.$$

As we intend to make use of the theory developed in Barndorff-Nielsen et al. (2009, 2011) we adopt the assumptions of those papers. The assumptions are standard in the literature on fractal processes and are as follows.

(A1) For some $\alpha \in \left(-\frac{1}{2}, \frac{1}{2}\right)$,

$$\gamma_2(x) = x^{2\alpha+1} L(x), \quad x \in (0, \infty), \tag{2.1}$$

where $L : (0, \infty) \to [0, \infty)$ is continuous. The function L is assumed to be slowly varying at zero, in the sense that $\lim_{x \to 0} \frac{L(tx)}{L(x)} = 1$ for all $t > 0$.

(A2) $\frac{d^2}{dx^2}\gamma_2(x) = x^{2\alpha-1} L_2(x)$ for some slowly varying (at zero) function L_2, which is continuous on $(0, \infty)$.[1]

[1] Following Bennedsen et al. (2016) this assumption is replaced by the following in the case $\alpha = 0$: (A2') $\frac{d^2}{dx^2}\gamma_2(x) = f(x) L_2(x)$, where L_2 is as in (A2), and the function f is such that $|f(x)| \leq C x^{-\beta}$ for some constants $C > 0$ and $\beta > 1/2$.

(A3) There exists $b \in (0,1)$ with

$$\limsup_{x\to 0} \sup_{y\in[x,x^b]} \left| \frac{L_2(y)}{L(x)} \right| < \infty.$$

Remark 2.1. The technical assumption (A3) can be replaced by the weaker assumption

$$\left| \frac{\gamma_2((j+1)/n) - 2\gamma_2(j/n) + \gamma_2((j-1)/n)}{2\gamma_2(1/n)} \right| \leq r(j), \quad \frac{1}{n}\sum_{j=1}^{n} r(j)^2 \to 0, \quad n \to \infty,$$

for some sequence $r(j)$.

The parameter $\alpha \in (-1/2, 1/2)$ is called the *fractal index* or *roughness index* of X, since the value of α reflects itself in the *pathwise properties* of X, as the following result formalizes.

Proposition 2.1. *Let X be a Gaussian process with stationary increments satisfying (A1) with fractal index $\alpha \in (-1/2, 1/2)$. Then there exists a modification of X which has Hölder continuous trajectories of order ϕ for all $\phi \in \left(0, \alpha + \frac{1}{2}\right)$.*

Remark 2.2. Proposition 2.1, as well as most of the asymptotic theory developed in the statistical literature on the fractal index, takes its departure point in (stationary) Gaussian processes. However, the theory, and also the bootstrap method in this paper, is valid more generally. For instance, the scaling relationship (2.1) and its implications for the pathwise properties of X as expounded in Proposition 2.1 is not only applicable to Gaussian processes, see Constantine and Hall (1994) and the discussion in Davies and Hall (1999). We explicitly consider the extension to non-Gaussian processes in Section 4.

Proposition 2.1 shows that α controls the degree of (Hölder) continuity of X. In particular, negative values of α corresponds to X having very *rough* paths, while positive values of α corresponds to *smooth* paths. It is well known that the Brownian motion has $\alpha = 0$. Indeed, $\alpha = 0$ is a necesssary condition for X to be a semimartingale, as shown in Section 2.1. An example of the kind of processes we have in mind is the *Cauchy process*.

Example 2.1 (Cauchy process, Gneiting and Schlather (2004))**.** Let X be the zero-mean, unit variance, stationary Gaussian process with correlation function

$$\rho(h) = \left(1 + |h|^{2\alpha+1}\right)^{-\frac{\beta}{2\alpha+1}}, \quad h \in \mathbb{R},$$

with $\alpha \in (-1/2, 1/2)$ and $\beta > 0$. We will call such a process the Cauchy process. As shown in Barndorff-Nielsen et al. (2009) Example 3, the Cauchy process fulfills assumptions (A1)–(A3).

To get an intuitive understanding of how the trajectories of the fractal processes look, and in particular how the value of α reflects itself in the roughness of the paths, Figure 1 plots three simulated trajectories of the Cauchy process. It is evident how negative values of α correspond to very rough paths, while the paths become smoother as α increases.

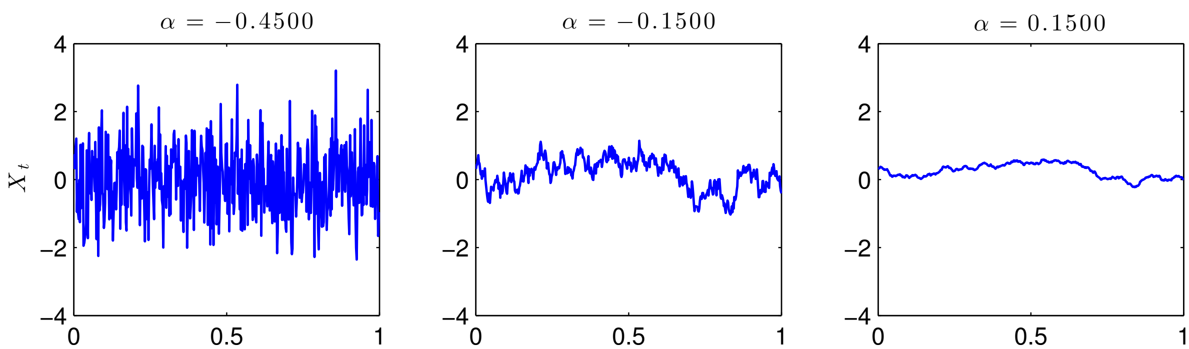

Figure 1: *Simulations of the unit-variance Cauchy process of Example 2.1 with* $\beta = 0.75$*,* α *as indicated above the plots, and* $n = 500$ *observations on the unit interval. The same random numbers were used for all three instances.*

2.1 Testing for non-semimartingality

Fractal processes with $\alpha \neq 0$ are not semimartingales, which implies that the null hypothesis $H_0 : \alpha = 0$ can be used to test whether a process is a non-semimartingale. In Appendix A the following basic fact is shown.

Proposition 2.2. *Let* X *be a Gaussian process with stationary increments satisfying (A1) with fractal index* $\alpha \in \left(-\frac{1}{2}, 0\right) \cup \left(0, \frac{1}{2}\right)$*. Then,* X *is not a semimartingale.*

Together with bootstrap procedure 1 presented below, this proposition will be the basis of our test for non-semimartingality by testing null hypotheses of the form $H_0 : \alpha = 0$.

3 Semiparametric estimation and bootstrapping of the fractal index

Consider n equidistant observations $X_{1/n}, X_{2/n}, \ldots, X_1$ of the stochastic process X, observed over a fixed time interval, which we without loss of generality take to be the unit interval, so that the time between observations is $\Delta_n := \frac{1}{n}$. As $n \to \infty$, this gives rise to the so-called *in-fill asymptotics*. In what follows, suppose that the process X satisfies the assumptions (A1)–(A3).

When X is Gaussian, it holds, by standard properties on the (absolute) moments of the Gaussian distribution and (2.1), that

$$\gamma_p(h) = C_p |h|^{(2\alpha+1)p/2} L_p(h), \tag{3.1}$$

where L_p is slowly varying at zero and $C_p > 0$ is a constant. This motivates the regression

$$\log \hat{\gamma}_p(h) = c_p + a \log |h| + U_h + \epsilon_h, \quad h = \frac{1}{n}, \frac{2}{n}, \ldots, \frac{m}{n}, \tag{3.2}$$

where $p > 0$, $m \in \mathbb{N}$ is a bandwidth parameter,

$$c_p = \log C_p, \quad a = \frac{(2\alpha+1)p}{2}, \quad U_h = \log\left(\frac{\hat{\gamma}_p(h)}{\gamma_p(h)}\right), \quad \text{and} \quad \epsilon_h = \log L_p(h).$$

The variogram γ_p is estimated straightforwardly as

$$\hat{\gamma}_p(k/n) := \frac{1}{n-k}\sum_{i=1}^{n-k} |X_{\frac{i+k}{n}} - X_{\frac{i}{n}}|^p, \quad k \geq 1, \tag{3.3}$$

and, given an estimate $\hat{a}$ of a from (3.2), the estimate of the fractal index is $\hat{\alpha} = \frac{\hat{a}}{p} - \frac{1}{2}$. This estimator is well known and well tested in the literature, e.g. Gneiting and Schlather (2004); Bennedsen (2015). The following proposition shows the consistency of the OLS estimator of α.

Proposition 3.1. *Suppose X is Gaussian and satisfies assumptions (A1)–(A3) with fractal index $\alpha \in (-1/2, 1/2)$. Fix $p > 0$, $m \in \mathbb{N}$ and let $\hat{\alpha} = \hat{\alpha}_{p,m}$ be the OLS estimator of α from (3.2). Now, as $n \to \infty$,*

$$\hat{\alpha} \xrightarrow{P} \alpha,$$

where "$\xrightarrow{P}$" refers to convergence in $\mathbb{P}$-probability.

A number of studies have considered the asymptotic properties of the OLS estimates coming from the regression (3.2), e.g. Constantine and Hall (1994), Davies and Hall (1999), and Coeurjolly (2001, 2008). For a brief summary of this literature, see Gneiting et al. (2012), Section 3.1. The following theorem presents the details when X is a Gaussian process satisfying (A1)–(A3). It holds for $\alpha \in (-1/2, 3/4)$ and the asymptotic variance is infeasible to calculate when $p \neq 2$.

Theorem 3.1. *Suppose X is Gaussian and satisfies assumptions (A1)–(A3) with fractal index $\alpha \in (-1/2, 1/4)$. Fix $m \in \mathbb{N}$ and let $\hat{\alpha} = \hat{\alpha}_{p,m}$ be the OLS estimator of α from (3.2). Now, as $n \to \infty$,*

$$\sqrt{n}(\hat{\alpha} - \alpha) \xrightarrow{d} Z_p, \qquad Z_p \sim N\left(0, \sigma^2_{m,p}\right),$$

where

$$\sigma^2_{m,p} = \frac{x_m^T \Lambda_p x_m}{(x_m^T x_m)^2 p^2},$$

with "T" denoting the transpose of a vector and x_m is the $m \times 1$ vector

$$x_m = \left(\log 1 - \overline{\log m}, \log 2 - \overline{\log m}, \ldots, \log m - \overline{\log m}\right)^T, \qquad \overline{\log m} := \frac{1}{m}\sum_{k=1}^{m} \log k,$$

and $\Lambda_p = \{\lambda_p^{k,v}\}_{k,v=1}^m$ is a real-valued $m \times m$ matrix with entries

$$\lambda_p^{k,v} = \lim_{n\to\infty} n \cdot Cov\left(\frac{\hat{\gamma}_p(k/n; B^H)}{\gamma_p(k/n; B^H)}, \frac{\hat{\gamma}_p(v/n; B^H)}{\gamma_p(v/n; B^H)}\right), \quad k, v = 1, 2, \ldots, m, \tag{3.4}$$

where $\hat{\gamma}_\cdot(\cdot; B^H)$ is given by (3.3) when the underlying process is a fractional Brownian motion with Hurst parameter $H = \alpha + \frac{1}{2}$, and similarly for $\gamma_p(\cdot; B^H)$.

Remark 3.1. The limit in (3.4) exists for $k, v = 1, \ldots, m$ by Breuer and Major (1983), Theorem 1. See also Remark 3.3. in Corcuera et al. (2013).

Remark 3.2. As mentioned in the introduction, a result similar to Theorem 3.1 holds for $\alpha \geq 1/4$ but with a different convergence rate and limiting distribution. When $\alpha = 1/4$, the convergence rate is $\sqrt{n}\log n$ and Z_p is zero-mean Gaussian with an asymptotic variance different from $\sigma^2_{m,p}$. When $\alpha > 1/4$ the convergence rate is $n^{1-2\alpha}$ and the distribution of Z_p is of the Rosenblatt type, see Taqqu (1979).

Remark 3.3. The most relevant setup for us when conducting asymptotic analysis is the case $m = 2$. In this case we have

$$\sigma^2_{m,p} = \frac{\lambda_p^{11} + \lambda_p^{22} - 2\lambda_p^{12}}{p^2 \log(2)^2}.$$

Further, for $p = 2$ we can calculate the matrix $\Lambda_p = \{\lambda_p^{k,v}\}_{k,v=1}^2$ explicitly. The details are given in Appendix B.

Perhaps surprisingly, Theorem 3.1 shows that the asymptotic distribution of the OLS estimator does not depend on the precise structure of the DGP of X, but only on the value of the fractal index α, through the correlation structure of the increments of an fBm with Hurst index $H = \alpha + 1/2$. The reason for this is that the small scale behavior of a process X fulfilling assumption (A1), will have the same small scale behavior as increments of the fBm. To see this, write

$$\begin{aligned} r_n(j) &:= Corr\left(X_{\frac{j+1}{n}} - X_{\frac{j}{n}}, X_{\frac{1}{n}} - X_0\right) \\ &= \frac{\gamma_2((j+1)/n) - 2\gamma_2(j/n) + \gamma_2((j-1)/n)}{2\gamma_2(1/n)} \\ &\to \frac{1}{2}\left(|j+1|^{2\alpha+1} - 2|j|^{2\alpha+1} + |j-1|^{2\alpha+1}\right), \quad n \to \infty, \end{aligned} \tag{3.5}$$

by assumption (A1) and the properties of slowly varying functions. We recognize (3.5) as the correlation function of the incremtents of an fBm with Hurst index $H = \alpha + 1/2$. As shown in the proof of Theorem 3.1, this will imply that the asymptotic variance of the estimator, $\sigma^2_{m,p}$, is the same for *all* Gaussian processes fulfilling assumptions (A1)–(A3), including the fBm. This fact will be the basis of our Monte Carlo algorithm: we will approximate the asymptotic distribution of Z_p using a fractional Brownian motion and, by Theorem 3.1, this will allow us to conduct correct inference, even though the DGP of X itself might be very different from the fBm.

Theorem 3.1, and the discussion preceeding it, alludes to some of the problems with asymptotic analysis for conducting inference on α in the general, semiparametric, setting (2.1). Some advantages of a simulation-based approach, as compared to asymptotic analysis include:

1. Our methods trivially allow for any $p > 0$. In contrast, a general and feasible asymptotic theory seems to be lacking in this case (although see Coeurjolly, 2001). For instance, the calculation of Λ_p in Theorem 3.1, cf. (3.4), appears to be infeasible for $p \neq 2$. Having an approach that allows for any $p > 0$ is desirable, as other values, e.g. $p = 1/2$ or $p = 1$, has been shown to be preferable to use in some cases. In particular, Gneiting et al. (2012) recommend using $p = 1$, as this choice is robust to outliers in the data, while Corcuera et al. (2013) recommend using several values for p for checking the robustness of $\hat{\alpha}$.

2. It is well known that the asymptotic distribution of the OLS estimator (3.2) of α is Gaussian for $\alpha \in (-1/2, 1/4]$, but non-standard for $\alpha > 1/4$. In the latter case, the distribution is given by the Rosenblatt distribution, as outlined in Taqqu (1975). As explained in Remark 3.2, the convergence rate is also different depending on the true value of α. This is the reason for assuming $\alpha \in (-1/2, 1/4)$ in Theorem 3.1. In contrast, we find that our Monte Carlo approach works well for the whole range $\alpha \in (-1/2, 1/2)$. This is because this approach directly approximates the distribution of $\hat{\alpha} - \alpha$, i.e. it automatically replicates any non-Gaussianity in the limiting distribution, induced by values of α larger than $1/4$, as well as differing convergence rates.

3. The methods of this paper are applicable and easily implemented for any choice of bandwidth parameter $m \geq 2$. In particular, implementation is not encumbered by choosing m large. In contrast, asymptotic theory is significantly more complex when $m \geq 3$; this is illustrated in Theorem 3.1, where the matrix Λ_p is an $m \times m$ matrix. This will allow us to investigate, through simulations, which value of m is preferred to use in practice. In Section 5 simulations will show that the root mean squared error of the OLS estimator of α is minimized for $m \geq 3$; also, when the sample size is moderate to large, choosing $m = 3$ or $m = 4$ will result in hypothesis tests with better size and power properties. These findings are in contrast with the conventional wisdom for asymptotic analysis, where it is usually recommended to let $m = 2$.

4. As mentioned in Section 3.1. of Gneiting et al. (2012), a general asymptotic theory for non-Gaussian X seems to be lacking. In Section 4.1, we will introduce non-Gaussianity of X, through volatility modulation, and show how our bootstrap approach is valid for a large class of non-Gaussian processes.

Two different bootstrap (or, more accurately, Monte Carlo) approaches, are detailed in the following two subsections. The idea behind the procedures is to simulate an auxiliary fractional process, an fBm, and estimate the fractal index of this process using (3.2) and then perform this operation $B \in \mathbb{N}$ times to approximate the distribution of $\hat{\alpha} - \alpha$. By Theorem 3.1 this approach will work no matter the actual DGP of X, as long as X is a Gaussian process satisfying (A1)–(A3). In other words, when X is Gaussian, we can use auxiliary fBms to estimate the distribution of Z_p in (1.2), *even though the DGP of X might be very different from the fBm.*

It turns out, however, that when X contains stochastic volatility (thus inducing non-Gaussianity of X) $\hat{\alpha}$ will have a limiting distribution which is different from the one which were described in Theorem 3.1. This is formalized in Theorem 4.1 below, where the volatility modulated Brownian semistationary process is introduced. For such processes, it is generally the case that $S_p \neq 1$ in (1.2) and the distribution of Z_p thus needs to be corrected by this factor to obtain the correct distribution of $\hat{\alpha}$. For this purpose we propose the following simple estimator of S_p:

$$\widehat{S_p} = \frac{\sqrt{m_{2p}^{-1}\hat{\gamma}_{2p}(1/n)}}{m_p^{-1}\hat{\gamma}_p(1/n)}, \qquad m_s := \mathbb{E}[|U|^s], \quad U \sim N(0,1), \quad s > 0, \tag{3.6}$$

where $\hat{\gamma}_{\cdot}$ is defined in (3.3). The $\widehat{S_p}$ factor provides a "heteroskedasticity correction" and will be rigorously motivated in Theorem 4.1 below. In Appendix A the following is shown.

Proposition 3.2. *Suppose X is a Gaussian process satisfying (A1)–(A3). Let $p > 0$. Now,*

$$\widehat{S_p} \xrightarrow{P} 1, \quad n \to \infty.$$

Remark 3.4. The fBm fulfills the assumptions of Proposition 3.2.

Theorem 3.1 showed that when X does not contain heteroskedasticity, no correction by S_p is needed. Proposition 3.2 tells us that in these cases correction by $\widehat{S_p}$ is harmless asymptotically. We will see in Section 5 that correction by S_p is crucial to obtain valid inference using the bootstrap when the underlying DGP contains significant variability, e.g. because of the presence of stochastic volatility. In practice, we therefore recommend to always correct with $\widehat{S_p}$. In the algorithms and simulations below, bootstraps both without the correcting factor $\widehat{S_p}$ (termed "S^*") and with the correcting factor $\widehat{S_p}$ (termed "T^*") will be considered; we think of the latter as a studentized version of the former.

3.1 Bootstrap procedure 1

To test the hypothesis $H_0 : \alpha = \alpha_0$ for some $\alpha_0 \in \left(-\frac{1}{2}, \frac{1}{2}\right)$ consider the following bootstrap approach:

1. Estimate $\hat{\alpha}$ using the OLS regression in (3.2).
2. Compute $S = \hat{\alpha} - \alpha_0$ and $T = (\hat{\alpha} - \alpha_0)/\widehat{S_p}$, where $\widehat{S_p}$ is given by (3.6).
3. For $b = 1, 2, \ldots, B$.
   (a) Simulate n observations of an fBm with Hurst index $H^* = \alpha_0 + \frac{1}{2}$.
   (b) Estimate $\hat{\alpha}_b^*$ from the path of this fBm using the OLS regression in (3.2).
   (c) Compute $R_b^* = \hat{\alpha}_b^* - \alpha_0$.
4. Compare S and T with the appropriate percentile of $\{R_b^*\}_{b=1}^B$. P-values can be obtained by determining the relative position of S or T in the sorted version of $\{R_b^*\}_{b=1}^B$.

3.2 Bootstrap procedure 2

Instead of the above, consider the following bootstrap procedure which is more appropriate when one wishes to compute confidence intervals for $\hat{\alpha}$.

1. Estimate $\hat{\alpha}$ using the OLS regression in (3.2).
2. Compute $S = \hat{\alpha} - \alpha_0$ and $T = (\hat{\alpha} - \alpha_0)/\widehat{S_p}$, where $\widehat{S_p}$ is given by (3.6).
3. For $b = 1, 2, \ldots, B$.
   (a) Simulate n observations of an fBm with Hurst index $H^* = \hat{\alpha} + \frac{1}{2}$.

(b) Estimate $\hat{\alpha}_b^*$ from the path of this fBm using the OLS regression in (3.2).

(c) Compute $R_b^* = \hat{\alpha}_b^* - \hat{\alpha}$.

4. Compare S and T with the appropriate percentiles of $\{R_b^*\}_{b=1}^B$. To obtain confidence intervals at the level $1-\delta$, e.g. a 95% confidence interval for $\delta = 0.05$, one computes

$$CI_{1-\delta/2}^S = \left[\hat{\alpha} - R^*_{(1-\delta/2)}, \hat{\alpha} - R^*_{(\delta/2)}\right],$$

or

$$CI_{1-\delta/2}^T = \left[\hat{\alpha} - \widehat{S_p} \cdot R^*_{(1-\delta/2)}, \hat{\alpha} - \widehat{S_p} \cdot R^*_{(\delta/2)}\right],$$

where $R^*_{(x)}$ is the x'th empirical percentiles of $\{R_b^*\}_{b=1}^B$, and where $\widehat{S_p}$ were calculated in step 2.

Remark 3.5. In bootstrap procedure 1, the bootstrap auxiliary variables are generated under H_0 by setting $\alpha = \alpha_0$. This will minimize the probability of a Type I error, i.e. rejection of H_0 when H_0 is true (Davidson and MacKinnon, 1999). We therefore expect this method to result in superior size properties of the hypothesis test as compared to procedure 2.

4 Extensions

This section gives two extensions to the theory discussed above. First the case of non-Gaussianity, through volatility modulation of X, is considered and then the case where the increments of X are non-stationary.

4.1 Extension to stochastic volatility processes

A flexible way to introduce non-Gaussianity of processes for which the theory of the fractal index continues to hold is through volatility modulation. A very convenient process for this purpose is the *Brownian semistationary process.*

4.1.1 Brownian semistationary process

Let X be the (volatility modulated) Brownian semistationary ($\mathcal{BSS}$) process (Barndorff-Nielsen and Schmiegel, 2007, 2009),

$$X_t = \int_{-\infty}^t g(t-s)\sigma_s dW_s, \quad t \geq 0,$$

where W is a Brownian motion on $\mathbb{R}$, $\sigma = \{\sigma_t\}_{t\in\mathbb{R}}$ a stationary process, and g a Borel measurable function such that $\int_{-\infty}^t g(t-s)^2\sigma_s^2 ds < \infty$ a.s. See Appendix C.1 for details of the $\mathcal{BSS}$ process and Appendix C.1.1 for the specifications of the stochastic volatility process σ considered in this paper.

When σ is a stochastic process, the marginal distribution of X will be non-Gaussian; indeed, by conditioning on σ, it is seen that the marginal distribution of X is a *normal mean-variance mixture*:

$$X_t|(\sigma_s, s \leq t) \sim N\left(0, \int_0^\infty g(x)^2 \sigma_{t-x}^2 dx\right), \quad t \geq 0.$$

This is a convenient way of extending the theory of fractal processes beyond the Gaussian framework, encompassing a large class of non-Gaussian models. For instance, Barndorff-Nielsen et al. (2013) show that for a particular choice of kernel function g and stochastic volatility process σ, X will have a marginal distribution of the ubiquitous Normal Inverse Gaussian type.

The kernel function gives the $\mathcal{BSS}$ framework great flexibility. A particularly useful kernel function which have been applied in a number of studies, e.g. Barndorff-Nielsen et al. (2013) and Bennedsen (2015), is the so-called *gamma kernel*.

Example 4.1 (Γ-$\mathcal{BSS}$ process)**.** Let g be the gamma kernel, i.e. $g(x) = x^\alpha e^{-\lambda x}$ for $\alpha \in (-1/2, 1/2)$ and $\lambda > 0$. The resulting process

$$X_t = \int_{-\infty}^t (t-s)^\alpha e^{-\lambda(t-s)} \sigma_s dW_s, \quad t \geq 0,$$

is called the (volatility modulated) Γ-$\mathcal{BSS}$ process. This process has fractal index α and, in particular, the Matérn autocorrelation function (Matérn, 1960; Handcock and Stein, 1993). See Barndorff-Nielsen (2012, 2016) for studies of the gamma kernel.

If the theory considered in this paper is to hold for $\mathcal{BSS}$ processes, some technical assumptions on the kernel function g are required. These assumptions hold trivially for our main example, the gamma kernel of Example 4.1, and are as follows.

(A4) It holds that

(a) $g(x) = x^\alpha L_g(x)$, where L_g is slowly varying at zero.

(b) $g'(x) = x^{\alpha-1} L_{g'}(x)$, where $L_{g'}$ is slowly varying at zero, and, for any $\epsilon > 0$, we have $g' \in L^2((\epsilon, \infty))$. Also, for some $a > 0$, $|g'|$ is non-increasing on the interval (a, ∞).[2]

(c) For any $t > 0$,

$$F_t := \int_1^\infty |g'(x)|^2 \sigma_{t-x}^2 dx < \infty.$$

Another requirement is that the modulating process $\sigma = \{\sigma_t\}_{t \in \mathbb{R}}$ not be "too rough". As in Corcuera et al. (2013), the following assumption is therefore introduced.

(A5) For any $q > 0$, it holds that

$$\mathbb{E}[|\sigma_t - \sigma_s|^q] \leq C_q |t-s|^{\gamma q}, \quad t, s \in \mathbb{R},$$

for some $\gamma > 0$ and $C_q > 0$. For a power parameter $p > 0$, cf. equation (3.1), we further require that $\gamma \cdot \min\{p, 1\} > 1/2$.

[2]Again following Bennedsen et al. (2016), in the case $\alpha = 0$ an alternative assumption is adopted: (A5b') $g'(x) = L_{g'}(x)$, where $L_{g'}$ is as in (A4b).

Remark 4.1. In Bennedsen et al. (2015) it was shown that $\mathcal{BSS}$ processes satisfying (A1)–(A5) will have the same fractal and continuity properties as their Gaussian counterparts. That is, for such a $\mathcal{BSS}$ process Propositions 2.1 and 2.2 continues to hold. In other words, X will have a modification with Hölder continuous trajectories of order ϕ for all $\phi \in (0, \alpha + 1/2)$ and X will be a non-semimartingale when $\alpha \neq 0$.

Processes of the $\mathcal{BSS}$ type have been extensively studied recently. In particular, using theory developed in Barndorff-Nielsen et al. (2009, 2011, 2013) and Corcuera et al. (2013) we can prove the following $\mathcal{BSS}$ analogue to the Gaussianity-based CLT result in Theorem 3.1.[3]

Theorem 4.1. *Suppose X is a $\mathcal{BSS}$ process satisfying (A1)–(A5). Fix $p > 0$, $m \in \mathbb{N}$ and let $\hat{\alpha} = \hat{\alpha}_{p,m}$ be the OLS estimator of α from (3.2). Now, as $n \to \infty$,*

$$\sqrt{n}(\hat{\alpha} - \alpha) \xrightarrow{st} Z_p \cdot S_p, \qquad Z_p \sim N\left(0, \sigma^2_{m,p}\right),$$

where $\sigma^2_{m,p}$ is as in Theorem 3.1 and

$$S_p = \frac{\sqrt{\int_0^1 \sigma_s^{2p} ds}}{\int_0^1 \sigma_s^p ds}.$$

Here "st" denotes stable convergence (in law), see e.g. Rényi (1963).

Remark 4.2. Theorem 4.1 is similar to Theorem 3.1 except that the limiting distribution now has a heteroskedasticity term, S_p. By Theorem 3.1. in Corcuera et al. (2013) it is not hard to deduce that

$$\widehat{S_p} = \frac{\sqrt{m_{2p}^{-1}\hat{\gamma}_{2p}(1/n)}}{m_p^{-1}\hat{\gamma}_p(1/n)} \xrightarrow{P} S_p, \quad n \to \infty,$$

where $\widehat{S_p}$ is given by (3.6). This fact provides the theoretical justification for the choice of $\widehat{S_p}$ in the bootstrap algorithms in Section 3. Further, the stable convergence result of Theorem 4.1 allows us to deduce that,

$$\sqrt{n}\frac{\hat{\alpha} - \alpha}{\widehat{S_p}\sqrt{\sigma^2_{m,p}}} \xrightarrow{d} N(0,1), \quad n \to \infty,$$

which will be the basis of the CLT used for comparison with our Monte Carlo approach in the simulation study of Section 5. Recall that the factor $\sigma^2_{m,p}$ is only feasible to calculate when $p = 2$ and it gets increasingly cumbersome to calculate as m increases. We will therefore consider only the case with $p = 2$ and $m = 2$ when implementing the CLT in the simulation exercise below. The details were given in Remark 3.3.

[3] Similarly, in the $\mathcal{BSS}$ framework, one can derive a consistency result, analogous to Proposition 3.1, valid for the whole range $\alpha \in (-1/2, 1/2)$. The proof is similar to the one from Proposition 3.1; we therefore skip the details.

The $\mathcal{BSS}$ process introduced above is ideal for including stochastic volatility (SV) in the process. However, it is also possible to include SV in processes based on other Gaussian processes, such as the Cauchy process of Example 2.1. For instance, consider processes of the form

$$X_t = X_0 + \int_0^t \sigma_s dG_s, \quad t \geq 0, \tag{4.1}$$

where σ is a SV process and G is a fractal Gaussian process with centered and stationary increments, e.g. a Gaussian $\mathcal{BSS}$ process, an fBm, a Cauchy process, etc. The theory of Barndorff-Nielsen et al. (2009), and therefore also the bootstrap methods of this paper, holds also for such processes.

4.2 Extension to processes with non-stationary increments

When the increments of X are non-stationary an approach similar to what was done in Bennedsen et al. (2015) can be adopted as follows. Define the time-dependent variogram

$$\gamma_p(h,t) := \mathbb{E}[|X_{t+h} - X_t|^p], \quad h,t \in \mathbb{R},$$

and, analogously to (2.1), assume that

$$\gamma_p(h,t) \sim C_{p,t}|h|^{(2\alpha+1)p/2}L(h), \quad t > 0, \quad h \downarrow 0, \tag{4.2}$$

where again $C_{p,t} > 0$, $\alpha \in \left(-\frac{1}{2}, \frac{1}{2}\right)$, and L is a slowly varying function at zero. The bootstrap methods considered in this paper also apply to such processes. An example is the truncated Brownian semistationary process.

Example 4.2 (Truncated $\mathcal{BSS}$ process, Bennedsen et al. (2015))**.** Let

$$X_t = X_0 + \int_0^t g(t-s)\sigma_s dW_s, \quad t \geq 0,$$

where $X_0 \in \mathbb{R}$, W is a Brownian motion, and σ a stochastic volatility process. Bennedsen et al. (2015) call such a process a *truncated* $\mathcal{BSS}$ ($\mathcal{TBSS}$) process. When X satisfies (A1)–(A5), Bennedsen et al. (2015) show that α is indeed the fractal index of X, in the sense of $\gamma_p(h,t)$ satisfying (4.2).

5 Simulation study

This section presents the results of a Monte Carlo simulation study where the various approaches to inference considered above are compared. Tables 1 and 2 contain results of the finite sample properties of the size and power of the hypothesis test $H_0 : \alpha = \alpha_0$ against the double-sided alternative $H_1 : \alpha \neq \alpha_0$. A number of different DGPs are considered: three Gaussian DGPs satisfying (A1)–(A3) and three $\mathcal{BSS}$ processes satisfying (A1)–(A5). The Gaussian processes are the fBm, the Cauchy process of Example 2.1, and the powered exponential process. The details on the latter process is given in Appendix C.4, where it is also shown that it indeed satisfies assumptions (A1)–(A3). The three versions of the $\mathcal{BSS}$ process are all with the gamma kernel, as given in Example 4.1, but encompassing three different stochastic volatility regimes: "NoSV" refers to the process without stochastic volatility, while "SV1F" and "SV2F" refer to the $\mathcal{BSS}$ process with one- and two-factor stochastic volatility, respectively. See also Appendix C.1.1. Especially SV2F induces very strong kurtosis in the stochastic volatility process. Further details of all DGPs considered in the Monte Carlo simulations are given in Appendix C.

When testing H_0 five different approaches are considered: the asymptotics-based inference of Theorem 4.1 (labeled CLT), un-studentized bootstrap inference (S_1^* and S_2^* for bootstrap method 1 and 2, respectively), and studentized bootstrap inference (T_1^* and T_2^* for bootstrap method 1 and 2, respectively). Table 1 contains size calculations, that is rejection rates of H_0 when H_0 is true. Table 2 contains power calculations of the test; we test $H_0 : \alpha = 0$ but now simulate under the alternative, with the true value of the fractal index α as indicated in the table. Here, the null hypothesis $H_0 : \alpha = 0$ is chosen because it seems to be the most empirically relevant, as it can be used to test for semimartingality, cf. Section 2.1.

The tables show that, generally, all methods perform well when $p = 2$ and $\alpha < 1/4$. For small sample sizes, the CLT has slight size distortions, while the bootstrap methods retain the nominal size. This fact was also found for a different estimator and CLT in Bennedsen et al. (2016). When SV is present, however, especially the two-factor SV process SV2F, the performance of the un-studentized bootstraps (S^* statistics) deteriorates. In contrast, both the CLT and the studentized bootstrap approach (T^* statistics) work very well and we conclude that studentization is crucial for accurate bootstrap inference, at least when stochastic volatility/heteroskedasticity is present in the data.

We experimented with different values of the power parameter p; although the CLT is infeasible for $p \neq 2$, the bootstrap methods work well for all values of $p > 0$. An illustration of this in the case of $p = 1$ is shown in the tables. As discussed in Section 3, the fact that the bootstrap methods provide accurate inference for all $p > 0$ is highly desirable, as different values of p can be used for estimation that is outlier-robust ($p = 1$ in particular, see also Section 6) and for checking the general robustness of an α estimate by considering several values for p.

The case where $\alpha > 1/4$ is also investigated. In particular, the tables show results for $\alpha = 3/8 = 0.3750$, where the limiting distribution is now non-Gaussian. In this case, the CLT is not valid. Bootstrap method 1 works very well but Bootstrap method 2 suffers from size distortions; this is likely because this latter method simulates the auxiliary bootstrap fBms with Hurst index $H^* = \hat{\alpha} + 0.5$. When, by normal variation in the OLS estimator, $\hat{\alpha} \leq 1/4$ is estimated from the observations of X, the asymptotic distribution of the auxiliary bootstrap estimator $\hat{\alpha}_b^*$ will therefore be Gaussian and lead to wrong inference. We conclude, that one should be wary of using bootstrap method 2, when the process under study is expected to be very smooth, i.e. when α is large.

5.1 Optimal choice of bandwidth parameter

It is an open question how to choose the bandwidth, m, optimally. For this reason we conduct a simulation experiment, shown in Figure 2, to shed some light on this. In (a) we plot the root mean squared error (RMSE) of the OLS estimator of α coming from (3.2), as a function of m. It

Table 1: *Rejection rates under H_0.*

DGP: Gaussian processes ($\alpha = -0.1250$; $p = 2$)

n	fBm					Cauchy ($\beta = 0.75$)					Powered exp. ($c = 0.5$)				
	CLT	S_1^*	T_1^*	S_2^*	T_2^*	CLT	S_1^*	T_1^*	S_2^*	T_2^*	CLT	S_1^*	T_1^*	S_2^*	T_2^*
20	0.087	0.051	0.078	0.083	0.108	0.118	0.055	0.082	0.072	0.098	0.100	0.052	0.078	0.082	0.110
40	0.071	0.056	0.068	0.089	0.098	0.074	0.056	0.071	0.083	0.096	0.068	0.049	0.065	0.081	0.097
80	0.061	0.052	0.058	0.068	0.075	0.072	0.056	0.060	0.069	0.074	0.067	0.051	0.057	0.066	0.071
160	0.055	0.051	0.052	0.059	0.062	0.058	0.050	0.053	0.055	0.058	0.054	0.046	0.053	0.053	0.060
320	0.050	0.050	0.049	0.053	0.054	0.058	0.053	0.054	0.055	0.059	0.053	0.052	0.057	0.059	0.060
640	0.049	0.048	0.048	0.049	0.049	0.053	0.046	0.048	0.048	0.049	0.050	0.046	0.048	0.046	0.047

DGP: Γ-$\mathcal{BSS}$ ($\alpha = -0.1250$, $\lambda = 1$; $p = 2$)

n	noSV					SV1F					SV2F				
	CLT	S_1^*	T_1^*	S_2^*	T_2^*	CLT	S_1^*	T_1^*	S_2^*	T_2^*	CLT	S_1^*	T_1^*	S_2^*	T_2^*
20	0.099	0.052	0.076	0.086	0.114	0.091	0.047	0.070	0.074	0.095	0.103	0.102	0.079	0.133	0.110
40	0.067	0.051	0.065	0.081	0.099	0.075	0.055	0.065	0.085	0.099	0.077	0.120	0.068	0.152	0.099
80	0.067	0.052	0.057	0.066	0.071	0.056	0.048	0.053	0.063	0.069	0.068	0.154	0.065	0.175	0.087
160	0.054	0.044	0.051	0.055	0.061	0.056	0.053	0.057	0.063	0.064	0.051	0.162	0.052	0.174	0.065
320	0.054	0.053	0.054	0.059	0.061	0.049	0.045	0.048	0.048	0.050	0.055	0.168	0.050	0.177	0.058
640	0.050	0.047	0.050	0.047	0.049	0.055	0.051	0.050	0.054	0.053	0.052	0.177	0.054	0.182	0.061

DGP: Γ-$\mathcal{BSS}$ ($\alpha = 0$, $\lambda = 1$; $p = 2$)

n	noSV					SV1F					SV2F				
	CLT	S_1	T_1	S_2	T_2	CLT	S_1	T_1	S_2	T_2	CLT	S_1	T_1	S_2	T_2
20	0.100	0.044	0.073	0.099	0.124	0.107	0.050	0.072	0.103	0.124	0.114	0.092	0.066	0.148	0.114
40	0.078	0.053	0.066	0.077	0.091	0.083	0.050	0.063	0.079	0.091	0.081	0.116	0.060	0.153	0.091
80	0.067	0.049	0.057	0.058	0.068	0.063	0.050	0.056	0.058	0.066	0.073	0.133	0.055	0.148	0.068
160	0.058	0.049	0.051	0.053	0.053	0.054	0.050	0.054	0.056	0.057	0.056	0.137	0.047	0.148	0.054
320	0.059	0.055	0.056	0.056	0.058	0.054	0.048	0.050	0.052	0.054	0.055	0.152	0.051	0.154	0.053
640	0.052	0.052	0.053	0.054	0.055	0.054	0.049	0.048	0.052	0.052	0.060	0.164	0.057	0.167	0.059

DGP: Γ-$\mathcal{BSS}$ ($\alpha = 0.3750$, $\lambda = 1$; $p = 2$)

n	noSV					SV1F					SV2F				
	CLT	S_1^*	T_1^*	S_2^*	T_2^*	CLT	S_1^*	T_1^*	S_2^*	T_2^*	CLT	S_1^*	T_1^*	S_2^*	T_2^*
20	–	0.059	0.079	0.078	0.096	–	0.051	0.069	0.072	0.090	–	0.139	0.114	0.175	0.147
40	–	0.055	0.066	0.065	0.077	–	0.061	0.070	0.076	0.087	–	0.161	0.109	0.193	0.134
80	–	0.059	0.065	0.079	0.084	–	0.052	0.060	0.073	0.081	–	0.170	0.095	0.219	0.129
160	–	0.051	0.058	0.082	0.089	–	0.060	0.066	0.096	0.101	–	0.164	0.076	0.219	0.129
320	–	0.052	0.057	0.098	0.101	–	0.052	0.055	0.098	0.102	–	0.159	0.067	0.228	0.114
640	–	0.054	0.056	0.106	0.112	–	0.059	0.062	0.117	0.116	–	0.142	0.052	0.220	0.110

DGP: Γ-$\mathcal{BSS}$ ($\alpha = -0.1250$, $\lambda = 1$; $p = 1$)

n	noSV					SV1F					SV2F				
	CLT	S_1^*	T_1^*	S_2^*	T_2^*	CLT	S_1^*	T_1^*	S_2^*	T_2^*	CLT	S_1^*	T_1^*	S_2^*	T_2^*
20	–	0.056	0.058	0.065	0.069	–	0.048	0.050	0.061	0.065	–	0.085	0.061	0.123	0.101
40	–	0.053	0.054	0.075	0.076	–	0.052	0.055	0.076	0.079	–	0.089	0.059	0.124	0.088
80	–	0.051	0.052	0.066	0.067	–	0.044	0.045	0.058	0.058	–	0.094	0.059	0.107	0.075
160	–	0.048	0.048	0.056	0.057	–	0.054	0.054	0.062	0.061	–	0.091	0.053	0.101	0.062
320	–	0.052	0.051	0.055	0.056	–	0.050	0.050	0.053	0.053	–	0.086	0.049	0.091	0.056
640	–	0.048	0.048	0.048	0.048	–	0.049	0.049	0.051	0.052	–	0.090	0.053	0.095	0.054

Finite sample size properties of the test $H_0 : \alpha = \alpha_0$ against $H_1 : \alpha \neq \alpha_0$ at a nominal size of 0.05. *The underlying DGP is simulated under H_0, i.e. the numbers in the table are the 'size' of the hypothesis test. The true parameter values used for the DGP, as well as the value of the power index p used for estimation, is given above the respective panels. For the CLT we choose the bandwidth $m = 2$, while the bootstrap methods set $m = 3$. 5 000 Monte Carlo runs, each with $B = 999$ bootstrap replications, were conducted.*

Table 2: *Rejection rates under H_1.*

DGP: Gaussian processes ($\alpha = -0.1250$; $p = 2$)

n	fBm					Cauchy ($\beta = 0.75$)					Powered exp. ($c = 0.5$)				
	CLT	S_1^*	T_1^*	S_2^*	T_2^*	CLT	S_1^*	T_1^*	S_2^*	T_2^*	CLT	S_1^*	T_1^*	S_2^*	T_2^*
20	0.209	0.084	0.118	0.127	0.156	0.275	0.128	0.168	0.165	0.205	0.233	0.096	0.132	0.131	0.163
40	0.264	0.163	0.185	0.192	0.215	0.313	0.233	0.255	0.266	0.285	0.266	0.183	0.203	0.214	0.230
80	0.365	0.306	0.322	0.314	0.328	0.440	0.398	0.413	0.401	0.413	0.391	0.336	0.347	0.340	0.353
160	0.584	0.583	0.590	0.574	0.581	0.655	0.668	0.673	0.663	0.664	0.608	0.610	0.614	0.607	0.614
320	0.850	0.886	0.885	0.882	0.880	0.885	0.923	0.923	0.920	0.920	0.862	0.902	0.904	0.897	0.899
640	0.989	0.996	0.995	0.996	0.996	0.991	0.997	0.997	0.997	0.996	0.989	0.996	0.996	0.996	0.995

DGP: Γ-$\mathcal{BSS}$ ($\alpha = -0.1250$, $\lambda = 1$; $p = 2$)

n	noSV					SV1F					SV2F				
	CLT	S_1^*	T_1^*	S_2^*	T_2^*	CLT	S_1^*	T_1^*	S_2^*	T_2^*	CLT	S_1^*	T_1^*	S_2^*	T_2^*
20	0.224	0.092	0.126	0.127	0.159	0.240	0.100	0.136	0.148	0.175	0.184	0.130	0.099	0.158	0.123
40	0.254	0.171	0.192	0.199	0.217	0.266	0.174	0.196	0.203	0.222	0.204	0.227	0.144	0.246	0.165
80	0.378	0.320	0.333	0.322	0.334	0.391	0.328	0.344	0.339	0.349	0.262	0.373	0.216	0.377	0.228
160	0.593	0.593	0.594	0.588	0.591	0.589	0.585	0.589	0.578	0.581	0.381	0.572	0.368	0.567	0.368
320	0.854	0.893	0.897	0.890	0.890	0.859	0.891	0.886	0.886	0.884	0.591	0.797	0.614	0.789	0.604
640	0.988	0.995	0.996	0.995	0.995	0.987	0.994	0.994	0.994	0.994	0.836	0.963	0.873	0.961	0.862

DGP: Γ-$\mathcal{BSS}$ ($\alpha = 0.3750$, $\lambda = 1$; $p = 2$)

n	noSV					SV1F					SV2F				
	CLT	S_1^*	T_1^*	S_2^*	T_2^*	CLT	S_1^*	T_1^*	S_2^*	T_2^*	CLT	S_1^*	T_1^*	S_2^*	T_2^*
20	–	0.460	0.515	0.632	0.659	–	0.443	0.495	0.611	0.639	–	0.371	0.336	0.498	0.479
40	–	0.842	0.848	0.895	0.898	–	0.839	0.842	0.889	0.892	–	0.711	0.613	0.777	0.716
80	–	0.991	0.989	0.994	0.994	–	0.992	0.991	0.994	0.994	–	0.938	0.871	0.951	0.903
160	–	1.000	1.000	1.000	1.000	–	1.000	1.000	1.000	1.000	–	0.997	0.982	0.997	0.987
320	–	1.000	1.000	1.000	1.000	–	1.000	1.000	1.000	1.000	–	1.000	0.999	1.000	1.000
640	–	1.000	1.000	1.000	1.000	–	1.000	1.000	1.000	1.000	–	1.000	1.000	1.000	1.000

DGP: Γ-$\mathcal{BSS}$ ($\alpha = -0.1250$, $\lambda = 1$; $p = 1$)

n	noSV					SV1F					SV2F				
	CLT	S_1^*	T_1^*	S_2^*	T_2^*	CLT	S_1^*	T_1^*	S_2^*	T_2^*	CLT	S_1^*	T_1^*	S_2^*	T_2^*
20	–	0.089	0.102	0.105	0.117	–	0.098	0.110	0.122	0.129	–	0.090	0.069	0.122	0.102
40	–	0.157	0.166	0.172	0.176	–	0.161	0.168	0.178	0.184	–	0.152	0.118	0.167	0.134
80	–	0.268	0.272	0.265	0.269	–	0.285	0.286	0.286	0.289	–	0.262	0.203	0.264	0.202
160	–	0.523	0.522	0.516	0.515	–	0.498	0.500	0.496	0.496	–	0.481	0.397	0.473	0.386
320	–	0.832	0.830	0.821	0.818	–	0.824	0.821	0.811	0.810	–	0.758	0.682	0.750	0.674
640	–	0.980	0.979	0.979	0.979	–	0.982	0.982	0.981	0.980	–	0.968	0.940	0.964	0.938

Finite sample size properties of the test $H_0 : \alpha = \alpha_0$ against $H_1 : \alpha \neq \alpha_0$ at a nominal size of 0.05*. The underlying DGP is simulated under the alternative, i.e. the numbers in the table are the 'power' of the hypothesis test. The true parameter values used for the DGP, as well as the value of the power index p used for estimation, is given above the respective panels. For the CLT we choose the bandwidth $m = 2$, while the bootstrap methods set $m = 3$.* 5 000 *Monte Carlo runs, each with $B = 999$ bootstrap replications, were conducted.*

seems that the RMSE is minimized for $m = 4$ or $m = 5$, depending on the number of observations, although for $m \in \{3, 4, 5\}$ there is not much difference in RMSE. Note, that $m = 2$ results in a significantly higher RMSE, especially for the smaller sample sizes. In (b) we plot the standard deviation of the random variable Z_p, i.e. $\sigma_{m,p}$, for $p = 2$. This is computed from $B = 999$ simulations of an fBm: we simulate an fBm, estimate α by the OLS regression (3.2) and compute the (numerical) standard deviation of $\hat{\alpha}$ over the $B = 999$ instances. This process is repeated $MC = 5\,000$ times and the numbers for $\sigma_{m,p}$ used in the plot is the average over these MC values. The same conclusions hold for the standard deviation of Z_p as for RMSE. What is more, the magnitude of $\sigma_{m,p}$ is almost exactly equal to the corresponding RMSE, indicating that the bias in the estimator is negligible. In (c) and (d) the finite sample properties of the hypothesis test $H_0 : \alpha = \alpha_0$ as a function of m is explored. The power is maximized for $m \in \{3, 4, 5\}$ but somewhat lower for $m = 2$. Choosing $m \geq 3$ will result in size distortions for the test, as compared to $m = 2$, when the number of observations is small ($n = 40, 80$), but when there is a moderate number of observations, $n \geq 100$ say, choosing $m \in \{3, 4, 5\}$ will result in a hypothesis test with more accurate size, as compared to the case $m = 2$.

From these investigations we conclude that choosing a low value for the bandwidth m is prudent. It seems, however, that there are gains from choosing $m \geq 3$. This is definitely the case when moderately many observations are available but likely true for a small number of observations as well, cf. Figure 2 (a). In Figure 2 the DGP underlying the simulations is a $\mathcal{BSS}$ process, but the conclusions hold for other DGPs as well. In particular, we confirmed the results using the fBm (Appendix C.2), the Cauchy process (Appendix C.3) and the powered exponential process (Appendix C.4), for all values of $\alpha \in (-1/2, 1/2)$. This is slightly at odds with Davies and Hall (1999) where the authors found, in simulations, that the mean squared error of $\hat{\alpha}$ was minimized for $m = 2$ when the DGP is the powered exponential process.

We recommend choosing $m = 3$ or $m = 4$, which seems to offer a good tradeoff between bias and variance. Choosing $m = 2$ essentially amounts to estimating α by drawing a straight line between only two points, $\log \hat{\gamma}_p(1/n)$ and $\log \hat{\gamma}_p(2/n)$, when running the OLS regression in (3.2). While this is tempting from a bias viewpoint – the scaling relationship (2.1) is only assumed to hold for small lag values – it seems to introduce more variance by relying on just two points.[4] However, because the bias is very small, it makes sense to focus on reducing variance, which is done by using more points to draw the line, i.e. choosing $m \geq 3$.

6 Empirical application: testing the semimartingale assumption on financial time series

This section studies price data from the Trades and Quote (TAQ) Database; in total, 29 different U.S. stocks, which are identified by their ticker symbol in Table 3, are analyzed. The data is sampled at a daily frequency: the log-price is the closing price on each day, while the volatility measure is the daily Realized Kernel (RK, Barndorff-Nielsen et al., 2008), constructed from intraday, high-frequency, returns. See Barndorff-Nielsen et al. (2009) for implementation of the RK. The data

[4]The point about bias being increasing in m was also made in Constantine and Hall (1994).

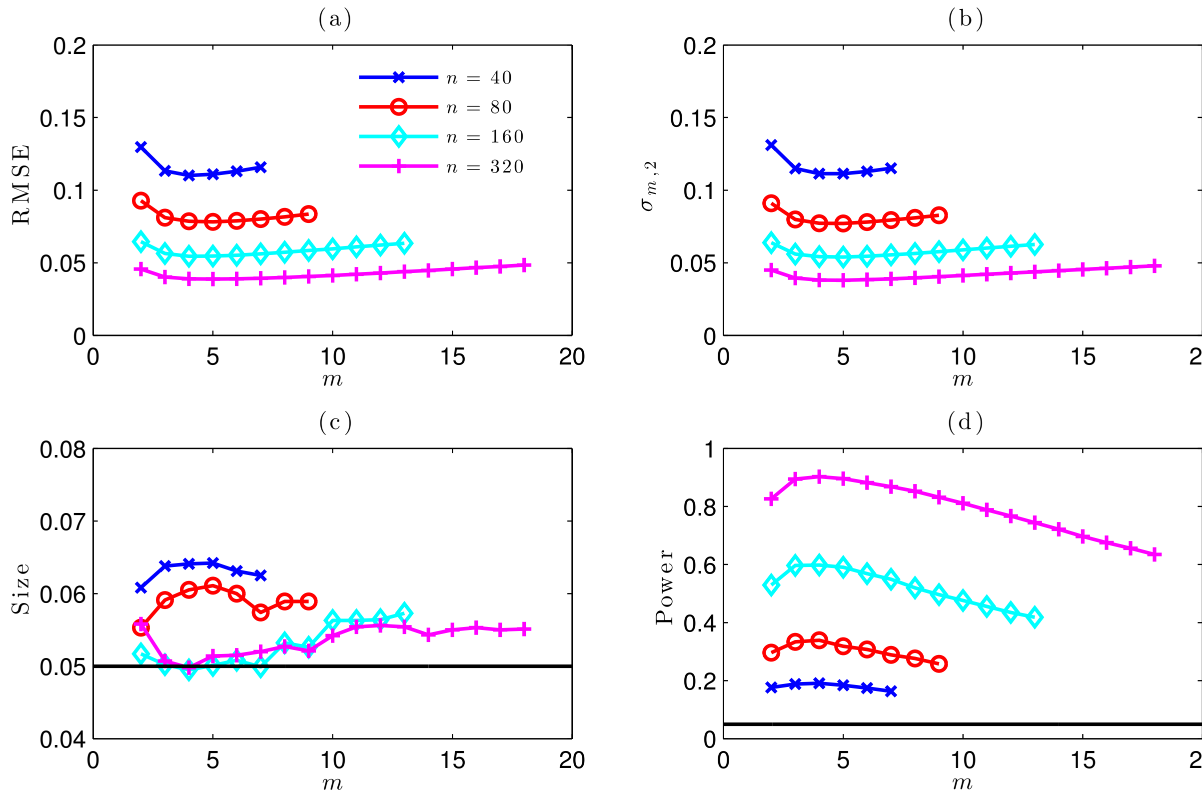

Figure 2: *Investigations of the impact of the bandwidth parameter m. (a): Root mean squared error (RMSE) of the OLS estimator of α from* (3.2)*. (b): The standard deviation of Z_p, $\sigma_{m,p}$, obtained by simulation of* 999 *replications of the fBm. (c): The size of the hypothesis test $H_0 : \alpha = -0.1250$ against the double sided $H_1 : \alpha \neq -0.1250$. (d): The power of the hypothesis test $H_0 : \alpha = 0$ against the double sided $H_1 : \alpha \neq 0$. The method for the tests is bootstrap procedure 1, using the T^* statistic with nominal size* 0.05*. We let $\alpha = -0.1250$, $p = 2$, $B = 999$, and perform* 5 000 *Monte Carlo replications. DGP: NoSV Γ-$\mathcal{BSS}$ with $\lambda = 1$ (see Appendix C.1).*

runs from January 2, 1997, until December 31, 2013, excluding weekends and holidays. For some assets, some days have been discarded due to limited trading during the day. All in all, we end up with an average of 4166 daily observations per asset.

For all data series we estimate α using the OLS regression (3.2), calculate 95% confidence intervals using bootstrap method 2, and calculate p-values for the null hypothesis $H_0 : \alpha = 0$ using bootstrap method 1. For the bootstraps we use the (studentized) T^* statistic. For the log-prices our alternative hypothesis is $H_1 : \alpha \neq 0$, while it for the log-volatility seems more relevant to choose H_1: $\alpha < 0$, to assess whether volatility is rough as has been conjectured.

In Section 6.3, we will pick out a particular asset, JPM (JPMorgan Chase), and investigate it in more depth, focusing in particular on the role of the power parameter p.

6.1 Application to log-prices

The application of the bootstrap methods of this paper to log-prices of financial assets can be motivated by the following stochastic volatility model. Let the stock price be denoted by $S = \{S_t\}_{t\geq 0}$, and suppose that its logarithm satisfies

$$\log S_t = \log S_0 + \int_0^t \sigma_s dG_s + A_t, \quad t \geq 0, \tag{6.1}$$

where $\sigma = \{\sigma_t\}_{t\geq 0}$ is a stochastic volatility process, $G = \{G_t\}_{t\geq 0}$ is a Gaussian process, such that the integral exists, and $A = \{A_t\}_{t\geq 0}$ is a smooth drift process, e.g. $A_t = -\frac{1}{2}\int_0^t \sigma_s^2 ds$. The most well-known instance of this model is of course the (Black-Scholes-type) case where $G = B$ is a Brownian motion, and this model has been extensively studied and has proven useful in many areas of economics and finance (see Shephard, 2005, for a book-length treatment). Although the model (6.1) includes a drift term A, this will not influence the estimation of α, as long as the process A is sufficiently smooth (see e.g. Lemma 3.5. of Corcuera et al., 2013).

Recall, that Proposition 2.2 showed that $\alpha \neq 0$ implies that the underlying process is *not* a semimartingale. Standard theory of asset prices states that log-prices which are not semimartingales will imply arbitrage opportunities, theoretically at least (Delbaen and Schachermayer, 1994). In what follows, we test the semimartingale null on log-prices using the approach outlined above.

The results are presented in Table 3. For all assets, the estimates of α are fairly close to 0, as one would expect under a no-arbitrage assumption. However, when $p = 2$ (left-most columns) there is huge variation in the estimator, as evidenced by the wide confidence intervals. Further, the average p-value is found to be quite large (0.81). The reason for this is most likely that the price data is not filtered for stock splits and mergers. Therefore, there may occasionally be large jumps in the quoted prices. This is illustrated for a particular stock in Section 6.3 (Figure 3) below, where we take a closer look at the JPM asset, but similar outliers are found in the time series of the other assets producing wide confidence intervals (not shown).

Outliers will bias estimates of α downwards and possibly invalidate any inference. Therefore, we also run the same exercise but with $p = 1$ (right-most columns of Table 3), which has been found to be robust to outliers in the data. In contrast to the former case, the confidence intervals are now fairly tight, indicating that the deteriorating effect of the stock splits and mergers are mitigated by choosing $p = 1$. What is more, when setting $p = 1$, estimates of α goes from being slightly negative to be scattered around zero, as seen in Table 3. Likewise, the average of the bootstrapped p-values is now 0.36, much closer to 0.50 which is the mean of the p-value if H_0 is true. This allows for much more precise inference, even in the presence of outliers, by choosing $p = 1$.[5] Recall, that in this case there is no feasible asymptotic theory available, so a Monte Carlo approach, such as presented in this paper, is the only viable option to the best of our knowledge.

Although $H_0 : \alpha = 0$ is rejected for 4 out of 29 assets (14%), these are likely false-positives given the 5% testing level. Indeed, the values of $\hat{\alpha}$ are very close to zero for these assets as well. We

[5] Of course, in practice a better approach would be to clean the data for stock splits and mergers before estimating α, but as our goal is to illustrate the advantages of using $p = 1$, we find that the experiment works best when these events are included.

conclude that there is no evidence of roughness/smoothness or non-semimartingality of the asset prices studied here.

6.2 Application to log-volatility

In this section, application of the bootstrap methods can be motivated from mathematical models of return volatility suggested previously in the finance/econometrics literature. In particular, consider the following simple stochastic volatility (Black-Scholes) model for the stock price S:

$$\frac{dS_t}{S_t} = \sigma_t dB_t, \quad t \geq 0, \tag{6.2}$$

where $\sigma = \{\sigma_t\}_{t\geq 0}$ is a stochastic volatility process and $B = \{B_t\}_{t\geq 0}$ a Brownian motion. The volatility process can be modeled as a log-fractal process, i.e.

$$\sigma_t = \exp(X_t), \quad t \geq 0,$$

where $X = \{X_t\}_{t\geq 0}$ is a stochastic process with fractal index $\alpha \in (-1/2, 1/2)$. Such a model was proposed in Comte and Renault (1996, 1998), where it was suggested that X is a fractional Brownian motion with fractal index $\alpha > 0$ (to allow for long memory). Conversely, Gatheral et al. (2014) suggested to model X by an fBm with $\alpha < 0$ (to allow for roughness). Most recently, Bennedsen et al. (2016) have proposed to model X by a $\mathcal{BSS}$ process with $\alpha < 0$, as this process can accommodate *both* roughness and long memory, in contrast to the fBm, which (by the self-similarity property) has either roughness or long memory but never both. Although these models have by now been much studied in the literature, so far little inference on α has been conducted. The present section therefore tests the semimartingale null for log-volatility by testing whether stochastic volatility is rough, i.e. running the hypothesis test $H_0 : \alpha = 0$ against the alternative $H_1 : \alpha < 0$.

Similar to the case of the log-prices, $\alpha < 0$ would imply, through Proposition 2.2, that volatility is a non-semimartingale. Contrary to the case of prices, however, such a fact would not imply arbitrage opportunities, since the log-prices themselves – even in the presence of non-semimartingale volatility – could still be semimartingales. This is for instance the case in the model (6.2) above.

The results are given in Table 4. We find $\hat{\alpha} \approx -0.33$, which is the overall mean of the estimates when $p = 2$. This is in line with what was found for similar time series in Gatheral et al. (2014) and Bennedsen et al. (2016). The test H_0: $\alpha = 0$ is rejected in favor of the alternative H_1: $\alpha < 0$ for all series for $p = 2$ as well as for $p = 1$. Also, the confidence intervals are tight in both cases, increasing our belief in the robustness of the results. In light of the findings for the log-prices above, it might also provide tentative evidence that there are not any (large) jumps in volatility.

In summary, we conclude that we find very strong evidence in favor of the recently advanced hypothesis that stochastic volatility is rough (Gatheral et al., 2014).

6.3 A closer look at the JPM stock

Let us now take a closer look at the JPM (JPMorgan Chase) asset, which was a case where the confidence bands were particularly wide when α was estimates from the log-prices with $p = 2$, cf.

Table 3: *Testing H_0: $\alpha = 0$ on log-prices.*

		$p=2$			$p=1$		
Asset	n	$\hat{\alpha}$	95% CI	p-value	$\hat{\alpha}$	95% CI	p-value
AA	4278	0.00	$(-0.14, 0.14)$	1.00	0.03	$(-0.00, 0.06)$	0.07
AIG	4277	0.03	$(-0.34, 0.42)$	0.89	0.07	$(0.02, 0.13)$	**0.00**
AXP	4277	-0.03	$(-0.25, 0.20)$	0.78	-0.01	$(-0.04, 0.02)$	0.38
BA	4277	-0.01	$(-0.16, 0.15)$	0.90	0.02	$(-0.01, 0.04)$	0.32
BAC	4277	0.01	$(-0.10, 0.12)$	0.85	0.02	$(-0.01, 0.05)$	0.17
C	4263	0.03	$(-0.38, 0.42)$	0.91	0.05	$(0.01, 0.10)$	**0.01**
CAT	4277	-0.01	$(-0.17, 0.16)$	0.96	0.05	$(0.02, 0.08)$	**0.00**
CVX	3078	-0.06	$(-0.32, 0.22)$	0.69	-0.02	$(-0.06, 0.01)$	0.20
DD	4278	-0.02	$(-0.20, 0.16)$	0.78	0.01	$(-0.02, 0.04)$	0.47
DIS	4278	-0.03	$(-0.32, 0.28)$	0.83	0.01	$(-0.03, 0.04)$	0.69
GE	4277	-0.00	$(-0.30, 0.28)$	0.98	0.02	$(-0.02, 0.05)$	0.28
GM	3906	-0.01	$(-0.56, 0.59)$	0.98	0.05	$(-0.01, 0.11)$	0.14
HD	4277	0.01	$(-0.12, 0.14)$	0.95	0.03	$(-0.00, 0.06)$	0.07
IBM	4277	-0.03	$(-0.26, 0.17)$	0.79	0.01	$(-0.02, 0.05)$	0.42
INTC	4277	-0.01	$(-0.17, 0.14)$	0.84	-0.00	$(-0.03, 0.03)$	0.99
JNJ	4277	-0.02	$(-0.29, 0.31)$	0.90	-0.00	$(-0.03, 0.03)$	0.95
JPM	4277	-0.05	$(-0.33, 0.25)$	0.72	-0.02	$(-0.05, 0.02)$	0.32
KO	4277	-0.00	$(-0.26, 0.26)$	0.98	0.01	$(-0.02, 0.04)$	0.40
MCD	4277	-0.02	$(-0.28, 0.28)$	0.91	0.02	$(-0.01, 0.05)$	0.32
MMM	4277	-0.02	$(-0.25, 0.24)$	0.83	0.01	$(-0.02, 0.04)$	0.64
MRK	4277	-0.02	$(-0.21, 0.19)$	0.88	0.02	$(-0.01, 0.05)$	0.21
MSFT	4277	-0.02	$(-0.20, 0.17)$	0.83	0.01	$(-0.02, 0.05)$	0.38
PG	4277	-0.02	$(-0.27, 0.26)$	0.88	-0.01	$(-0.05, 0.03)$	0.55
SPY	4278	-0.06	$(-0.09, -0.02)$	**0.00**	-0.01	$(-0.03, 0.02)$	0.59
T	4270	-0.01	$(-0.17, 0.14)$	0.94	0.02	$(-0.02, 0.05)$	0.30
UTX	4277	-0.01	$(-0.23, 0.21)$	0.94	-0.01	$(-0.04, 0.03)$	0.70
VZ	3394	-0.03	$(-0.07, 0.01)$	0.14	-0.02	$(-0.05, 0.00)$	0.10
WMT	4277	-0.01	$(-0.20, 0.17)$	0.94	-0.01	$(-0.03, 0.02)$	0.72
XOM	3542	-0.07	$(-0.31, 0.19)$	0.58	-0.05	$(-0.09, -0.02)$	**0.00**
Avg	4166	-0.02	$(-0.24, 0.22)$	0.81	0.01	$(-0.02, 0.04)$	0.36

Empirical investigations concerning the roughness properties of financial log-prices. Stocks are identified by their ticker symbol, with "Avg" being the mean over all assets. α is estimated with the OLS regression (3.2) with $m = 3$. The confidence intervals (CI) are computed using bootstrap method 2 with $B = 999$. The columns with "p-value" are simulated p-values using bootstrap method 1; bold face numbers denote rejections of $H_0 : \alpha = 0$ at a 5% level. The alternative is $H_1 : \alpha \neq 0$.

Table 4: *Testing H_0: $\alpha = 0$ on log-volatility.*

		$p = 2$			$p = 1$		
Asset	n	$\hat{\alpha}$	95% CI	p-value	$\hat{\alpha}$	95% CI	p-value
AA	4278	−0.36	(−0.39, −0.33)	**0.00**	−0.37	(−0.39, −0.34)	**0.00**
AIG	4277	−0.30	(−0.33, −0.27)	**0.00**	−0.31	(−0.33, −0.28)	**0.00**
AXP	4277	−0.33	(−0.35, −0.30)	**0.00**	−0.33	(−0.35, −0.30)	**0.00**
BA	4277	−0.33	(−0.36, −0.31)	**0.00**	−0.34	(−0.36, −0.31)	**0.00**
BAC	4277	−0.29	(−0.31, −0.26)	**0.00**	−0.27	(−0.30, −0.25)	**0.00**
C	4263	−0.31	(−0.34, −0.29)	**0.00**	−0.31	(−0.33, −0.28)	**0.00**
CAT	4277	−0.33	(−0.36, −0.31)	**0.00**	−0.32	(−0.34, −0.30)	**0.00**
CVX	3078	−0.30	(−0.33, −0.27)	**0.00**	−0.30	(−0.33, −0.27)	**0.00**
DD	4278	−0.34	(−0.37, −0.32)	**0.00**	−0.33	(−0.36, −0.31)	**0.00**
DIS	4278	−0.34	(−0.37, −0.32)	**0.00**	−0.35	(−0.38, −0.33)	**0.00**
GE	4277	−0.33	(−0.35, −0.31)	**0.00**	−0.33	(−0.35, −0.31)	**0.00**
GM	3906	−0.33	(−0.36, −0.31)	**0.00**	−0.34	(−0.36, −0.32)	**0.00**
HD	4277	−0.34	(−0.37, −0.31)	**0.00**	−0.33	(−0.35, −0.31)	**0.00**
IBM	4277	−0.33	(−0.35, −0.30)	**0.00**	−0.33	(−0.35, −0.30)	**0.00**
INTC	4277	−0.29	(−0.31, −0.26)	**0.00**	−0.29	(−0.31, −0.27)	**0.00**
JNJ	4277	−0.36	(−0.38, −0.34)	**0.00**	−0.35	(−0.38, −0.33)	**0.00**
JPM	4277	−0.31	(−0.34, −0.29)	**0.00**	−0.30	(−0.33, −0.28)	**0.00**
KO	4277	−0.35	(−0.37, −0.32)	**0.00**	−0.35	(−0.37, −0.33)	**0.00**
MCD	4277	−0.36	(−0.38, −0.33)	**0.00**	−0.35	(−0.37, −0.32)	**0.00**
MMM	4277	−0.34	(−0.37, −0.31)	**0.00**	−0.32	(−0.35, −0.30)	**0.00**
MRK	4277	−0.34	(−0.37, −0.32)	**0.00**	−0.35	(−0.37, −0.32)	**0.00**
MSFT	4277	−0.31	(−0.34, −0.29)	**0.00**	−0.31	(−0.33, −0.28)	**0.00**
PG	4277	−0.33	(−0.37, −0.30)	**0.00**	−0.34	(−0.36, −0.32)	**0.00**
SPY	4278	−0.30	(−0.32, −0.27)	**0.00**	−0.30	(−0.32, −0.27)	**0.00**
T	4270	−0.34	(−0.36, −0.31)	**0.00**	−0.33	(−0.35, −0.31)	**0.00**
UTX	4277	−0.35	(−0.38, −0.33)	**0.00**	−0.35	(−0.37, −0.32)	**0.00**
VZ	3394	−0.34	(−0.37, −0.31)	**0.00**	−0.33	(−0.35, −0.30)	**0.00**
WMT	4276	−0.38	(−0.40, −0.35)	**0.00**	−0.36	(−0.39, −0.34)	**0.00**
XOM	3542	−0.32	(−0.35, −0.29)	**0.00**	−0.32	(−0.34, −0.29)	**0.00**
Avg	4166	−0.33	(−0.36, −0.30)	0.00	−0.33	(−0.35, −0.30)	0.00

Empirical investigations concerning the roughness properties of financial log-volatility. Stocks are identified by their ticker symbol, with "Avg" being the mean over all assets. α is estimated with the OLS regression (3.2) with $m = 3$. The confidence intervals (CI) are computed using bootstrap method 2 with $B = 999$. The columns with "p-value" are simulated p-values using bootstrap method 1; bold face numbers denote rejections of $H_0 : \alpha = 0$ at a 5% level. The alternative is $H_1 : \alpha < 0$.

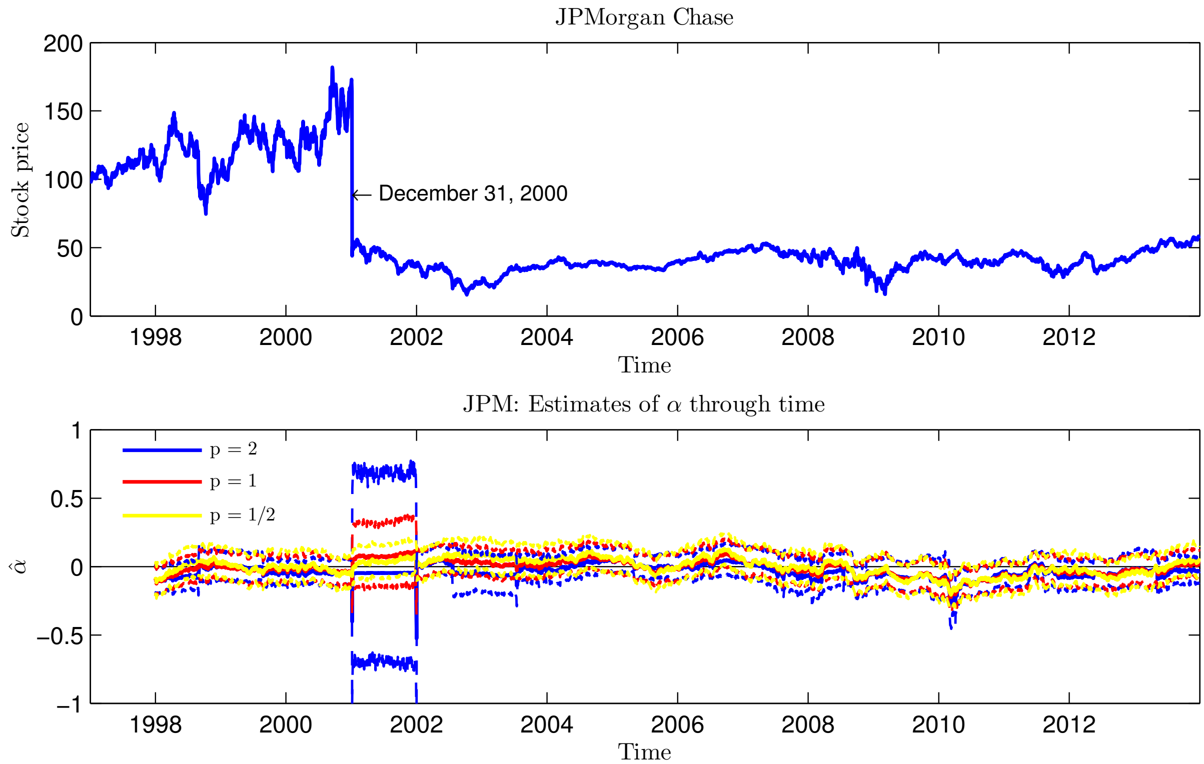

Figure 3: *Top: Stock price evolution of JPMorgan Chase (JPM) from January 2, 1997, until December 31, 2013. On December 31, 2000, J. P. Morgan & Co. merged with The Chase Manhattan Group. Bottom: Estimation of α in time by using a rolling window of* 250 *days and* $m = 3$*. Solid lines are estimates of α; dashed lines are* 95% *(point-wise) confidence bands calculated using the T^* statistic of bootstrap procedure 2 with* $B = 999$ *bootstrap replications.*

Table 3. The top plot of Figure 3 shows the (closing) price evolution of JPM from January 2, 1997 to December 31, 2013.

In the period under study, JPM has undergone several stock splits, which are not visible in the plot, and one large merger which is clearly visible. Indeed, on December 31st, 2000, J. P. Morgan & Co. merged with The Chase Manhattan Group causing a major change in the quoted price of the stock, as seen in the figure.

The effect of the large outlier in the JPM data is further analyzed in the bottom plot of Figure 3, where α is estimated from log-prices through time by using a rolling window with 250 days. It is evident how the confidence bands (dashed lines) get wide when the large outlier enters the data. This is alleviated somewhat by letting $p = 1$, and, to an even greater extend, when $p = 1/2$, thus providing further evidence that letting $p \leq 1$ will result in inference, which is more robust to outliers than $p = 2$.

This conclusion is strengthened in Figure 4, which shows estimates of α, as a function of p. In plot (a) the data is log-prices: it is clear how the values of $\hat{\alpha}$ is close to zero with tight confidence bands for $p \leq 1$, while the outlier will cause the estimate of α to be biased downwards, and the

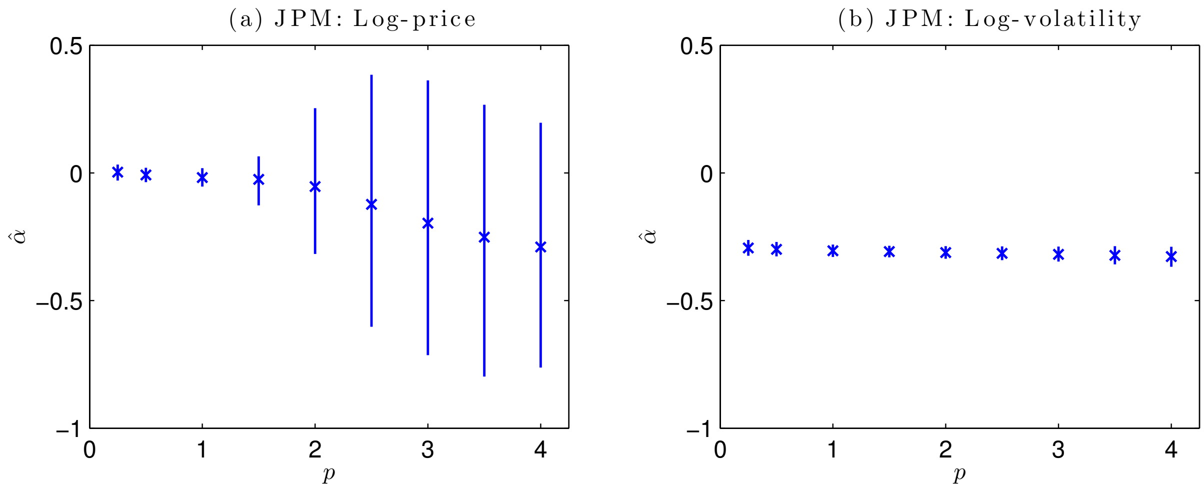

Figure 4: *Estimates of α (crosses) with associated 95% confidence bands (vertical lines) calculated using the T^* statistic of bootstrap procedure 2 with $m = 3$ and $B = 999$ bootstrap replications. The data is from the JPMorgan (JPM) stock as explained in the text. (a): log-prices. (b): log-volatility.*

confidence bands to be extremely wide, for $p > 1$. Conversely, in plot (b) the data is log-volatility: here the estimates of α are stable, as a function of p, and the confidence bands are very tight, as we would expect from such a large sample ($n = 4277$).

7 Conclusion

This paper has developed simulation-based methods to conduct inference on the fractal index of a time series. We considered a particular semiparametric estimator of the fractal index, based on OLS regression, but the same methods can be applied straightforwardly to different estimators of the fractal index, as long as the (asymptotic) distribution of the estimator does not rely on the particular characteristics on the DGP of the observations, but only on the fractal index α and a possible heteroskedasticity factor.

The paper also answers a call for a general approach to inference on α for non-Gaussian processes (Gneiting et al., 2012). Our methods allow for this, at least when the non-Gaussianity is *volatility induced*, which is the case in many applications of interest in (e.g.) economics, econometrics, and finance. In the empirical section, we considered two instances of such applications by looking at time series of log-prices and log-volatility. We saw that $p \leq 1$ will result in estimation and inference, which is more robust to outliers, as compared to $p > 1$. Semimartingale hypotheses were tested for the time series. Although no evidence of non-semimartingality was found in log-prices, strong evidence of non-semimartingality was found in log-volatility, thereby supporting the claim that volatility is rough (Gatheral et al., 2014).

A Proofs

Proof of Proposition 2.1. Note first, that since X is Gaussian Assumption (A1) implies that for $n \geq 1$,

$$\mathbb{E}[|X_t - X_s|^{2n}] = C_{2n}|t-s|^{(2\alpha+1)n}L(t-s)^{2n},$$

where $x \mapsto L(x)^{2n}$ is slowly varying at zero. Let now $K \subset (0,\infty)$ be a compact set. By the properties of slowly varying functions (Bingham et al., 1989, Theorem 1.5.6(ii)), for all $\epsilon > 0$ we can find $a > 0$ such that

$$E[|X_t - X_s|^{2n}] \leq \tilde{C}_{1,n}|t-s|^{1+(2\alpha+1)n-1-\epsilon}, \quad t, s \in (0, a],$$

for a constant $\tilde{C}_{1,n} > 0$. Suppose now that $t, s \in K$ such that $t - s > a$. Since L is continuous on $(0,\infty)$ we have that

$$E[|X_t - X_s|^{2n}] \leq \tilde{C}_{2,n}|t-s|^{1+(2\alpha+1)n-1},$$

for a constant $\tilde{C}_{2,n} > 0$. In summary, we have that there exists a constant $\tilde{C}_{3,n} > 0$ such that for all $\epsilon > 0$ we have

$$E[|X_t - X_s|^{2n}] \leq \tilde{C}_{3,n}|t-s|^{1+(2\alpha+1)n-1-\epsilon}, \quad t, s \in K.$$

Using this, we deduce that for n sufficiently large, the continuity criterion of Kolmogorov shows that X has a modification which is Hölder continuous of order ϕ for all $\phi \in \left(0, \frac{(2\alpha+1)n-1-\epsilon}{2n}\right) = \left(0, \alpha + 1/2 - \frac{1+\epsilon}{2n}\right)$. Letting $n \to \infty$ yields the desired result. ☐

Proof of Proposition 2.2. Recall the p-variation

$$V_p(0,T) := \sup_{\Pi} \sum_{j=1}^{n} |X_{t_j} - X_{t_{j-1}}|^p,$$

where the supremum is taken over all partitions with mesh going to zero. Consider the associated *index of p-variation*:

$$I(X, [0,T]) := \inf\{p > 0 | V_p(0,T) < \infty\}.$$

It is a well-known fact that semimartingales have $I(X, [0,T]) \in [0,1] \cup \{2\}$ with probability one. Likewise, it is known that if a process, X, has paths which are ϕ-Hölder continuous, then the index of p-variation is $\frac{1}{\phi}$ (e.g. Norvaiša, 2006). Now, by Proposition 2.1 we get that

$$p^* := I(X, [0,T]) = \frac{1}{\alpha + 1/2} \in (1,\infty) \setminus \{2\}.$$

In conclusion, X is therefore not a semimartingale. Note that $\alpha = 0 \Rightarrow p^* = 2$, so that the present result does not hold for $\alpha = 0$. ☐

Proof of Proposition 3.1. Note first, that since $\alpha = a/p - 1/2$ we can write

$$\hat{\alpha} - \alpha = \frac{1}{p x_m^T x_m} x_m^T (U^m + \epsilon^m), \tag{A.1}$$

where

$$U^m := \left(U_{1/n}, U_{2/n}, \ldots, U_{m/n}\right)^T = \left(\log\left(\frac{\hat{\gamma}_p(1/n)}{\gamma_p(1/n)}\right), \log\left(\frac{\hat{\gamma}_p(2/n)}{\gamma_p(2/n)}\right), \ldots, \log\left(\frac{\hat{\gamma}_p(m/n)}{\gamma_p(m/n)}\right)\right)^T,$$

and

$$\epsilon^m := \left(\epsilon_{1/n}, \epsilon_{2/n}, \ldots, \epsilon_{m/n}\right)^T = \left(\log L_p(1/n), \log L_p(2/n), \ldots, \log L_p(m/n)\right)^T.$$

To see that the term $x_m^T \epsilon^m$ vanishes, note that

$$\sum_{k=1}^{m} x_{m,k} = \sum_{k=1}^{m} \left(\log k - \overline{\log m}\right) = 0$$

and therefore

$$x_m^T \epsilon^m = \sum_{k=1}^{m} x_{m,k} \log L_p(k/n) = \sum_{k=1}^{m} x_{m,k} \log\left(\frac{L_p(k/n)}{L_p(1/n)}\right) \to 0, \quad n \to 0,$$

since $\lim_{n\to\infty} \frac{L_p(k/n)}{L_p(1/n)} = 1$ by the property of slowly varying functions.

The required result now follows by noting that

$$\frac{\hat{\gamma}_p(k/n)}{\gamma_p(k/n)} = \frac{\hat{\gamma}_p(k/n)}{m_p \gamma_2(k/n)^{p/2}} \xrightarrow{P} 1, \qquad n \to \infty, \quad k \geq 1,$$

by Propositon 1 in Barndorff-Nielsen et al. (2009). □

Proof of Theorem 3.1. Using Theorem 2 in Barndorff-Nielsen et al. (2011), see also Barndorff-Nielsen et al. (2009) Theorem 7, and the limit in equation (3.5), this paper, we get

$$\sqrt{n} \begin{pmatrix} \frac{\hat{\gamma}_p(1/n)}{\gamma_p(1/n)} - 1 \\ \vdots \\ \frac{\hat{\gamma}_p(m/n)}{\gamma_p(m/n)} - 1 \end{pmatrix} \xrightarrow{d} N(0, \Lambda_p), \quad n \to \infty, \tag{A.2}$$

where $\Lambda = \{\lambda_p^{k,v}\}_{k,v=1}^m$ is a $m \times m$ matrix with entries

$$\lambda_p^{k,v} = \lim_{n\to\infty} n \cdot Cov\left(\frac{\hat{\gamma}_p(k/n; B^H)}{\gamma_p(k/n; B^H)}, \frac{\hat{\gamma}_p(v/n; B^H)}{\gamma_p(v/n; B^H)}\right), \quad k, v = 1, 2, \ldots, m, \tag{A.3}$$

where $\gamma_p(\cdot; B^H)$ denotes the p'th order variogram for a fractional Brownian motion with Hurst index $H = \alpha + 1/2$, and similarly for $\hat{\gamma}_p$. Note that the limit in (A.3) exists for $k, v = 1, 2, \ldots m$, by Breuer and Major (1983), Theorem 1, see also Corcuera et al. (2013), Remark 3.3. Now, from (A.1) we get, using (A.2) and the delta method,

$$\sqrt{n}\,(\hat{\alpha} - \alpha) \xrightarrow{d} N\left(0, \frac{x_m^T \Lambda_p x_m}{(x_m^T x_m)^2 p^2}\right), \quad n \to \infty.$$

This concludes the proof. □

Proof of Proposition 3.2. Note that we can write

$$\widehat{S_p} = \frac{\sqrt{m_{2p}^{-1}\hat{\gamma}_p(1/n)/\gamma_2(1/n)^{2p}}}{m_p^{-1}\hat{\gamma}_p(1/n)/\gamma_2(1/n)^{p/2}}.$$

The result now follows from Proposition 1 in Barndorff-Nielsen et al. (2009). □

Proof of Theorem 4.1. Note first, that by Theorem 4 of Barndorff-Nielsen et al. (2011), see also Theorem 3.2. and Remark 3.4. of Corcuera et al. (2013), we get

$$\sqrt{n}\begin{pmatrix} \frac{\hat{\gamma}_p(1/n)}{\gamma_p(1/n)} - 1 \\ \vdots \\ \frac{\hat{\gamma}_p(m/n)}{\gamma_p(m/n)} - 1 \end{pmatrix} \xrightarrow{st} \int_0^1 \sigma_s^p \Lambda_p dBs,$$

where B is an m-dimensional Brownian motion, defined on an extension of the original probability space, $(\Omega, \mathcal{F}, \mathbb{P})$, independent of $\mathcal{F}$. The matrix Λ_p is identical to the one of Theorem 3.1, i.e. the covariances in Λ_p is calculated using the covariance structure of the fBm, not the $\mathcal{BSS}$ process.

We proceed as in the proof of Theorem 3.1. In particular, invoking the delta method we get

$$\sqrt{n}\,(\hat{\alpha} - \alpha) \xrightarrow{st} \frac{x_m^T \Lambda_p}{x_m^T x_m p} \frac{\int_0^1 \sigma_s^p dB_s}{\sigma_s^p ds},$$

or, in other words (conditionally on $\{\sigma_t\}_{t \in \mathbb{R}}$),

$$\sqrt{n}\,(\hat{\alpha} - \alpha) \xrightarrow{st} Z_p \cdot S_p, \quad S_p := \frac{\sqrt{\int_0^1 \sigma_s^{2p} ds}}{\int_0^1 \sigma_s^p ds},$$

and where Z_p is as in Theorem 3.1. This concludes the proof. □

B Deriving an expression for the Λ matrix of Theorem 3.1

Below we give expressions for the entries in the matrix $\Lambda_p = \{\lambda_p^{k,v}\}_{k,v=1}^2$ of Theorem 3.1 when $p = 2$. Let B^H be an fBm with Hurst index $H \in (0,1)$. Recall that

$$\gamma_2(k/n; B^H) := \mathbb{E}\left[\left|B_{k/n}^H - B_0^H\right|^2\right] = (k/n)^{2H}.$$

Therefore,

$$\lambda_2^{k,v} = \lim_{n\to\infty} n^{1+4H}(kv)^{-2H} Cov\left(\hat{\gamma}_2(k/n; B^H), \hat{\gamma}_2(v/n; B^H)\right), \quad k, v = 1, 2.$$

We illustrate how to derive the result using the case $k = 1$, $v = 2$ as example. Since B^H is Gaussian, we can use Isserlis' theorem to calculate (cross) moments of the increments of X. Brute force calculations yield

$$Cov\left(\hat{\gamma}_2(1/n; B^H), \hat{\gamma}_2(2/n; B^H)\right)$$

$$= \frac{1}{(n-1)(n-2)} Cov\left(\sum_{i=1}^{n-1} |X_{(i+1)/n} - X_{i/n}|^2, \sum_{j=1}^{n-1} |X_{(j+2)/n} - X_{j/n}|^2 \right)$$

$$= \frac{2^{-1} n^{-4H}}{(n-1)(n-2)} \sum_{i=1}^{n-1} \sum_{j=1}^{n-2} \left(|j-i+2|^{2H} - |j-i+1|^{2H} - |j-i|^{2H} + |j-i-1|^{2H} \right)^2,$$

where it was used that

$$\mathbb{E}[B^H_{i/n} B^H_{j/n}] = \frac{1}{2} n^{-2H} \left(|i|^{2H} + |j|^{2H} - |i-j|^{2H} \right),$$

since B^H is an fBm with Hurst index H. Now, deduce that

$$\lambda_2^{1,2} = 2^{-2H-1} \lim_{n\to\infty} n^{-1} \sum_{i=1}^{n-1} \sum_{j=1}^{n-2} \left(|j-i+2|^{2H} - |j-i+1|^{2H} - |j-i|^{2H} + |j-i-1|^{2H} \right)^2.$$

Similarly, it can be shown that

$$\lambda_2^{k,k} = 2^{-1} k^{-4H} \lim_{n\to\infty} n^{-1} \sum_{i=1}^{n-k} \sum_{j=1}^{n-k} \left(|j-i+k|^{2H} - 2|j-i|^{2H} + |j-i-k|^{2H} \right)^2, \quad k = 1, 2.$$

These expressions are convergent by Theorem 1 in Breuer and Major (1983), see also Remark 3.3. in Corcuera et al. (2013), but in our implementation we simply use the finite sample version by implementing the finite sums as given above.

C Simulation setup

Section 5 requires simulating $n \in \mathbb{N}$ equidistant observations of the process X on the unit interval $[0, 1]$. The following subsections give details concerning the various DGPs we consider for X. Simulation of the Gaussian DGPs can be done exactly using the Cholesky decomposition of the covariance matrix; since the processes are stationary (in case of the fBm the increments are stationary) one can get this covariance matrix from the correlation function ρ. When X contains stochastic volatility, the process is non-Gaussian and the Cholesky method is not valid. In this case, we use the *hybrid scheme* of Bennedsen et al. (2015) which is a fast and accurate simulation scheme for certain fractal processes with or without SV.

C.1 Brownian semistationary process

The Brownian semistationary ($\mathcal{BSS}$) process was introduced in Barndorff-Nielsen and Schmiegel (2007, 2009) and has been widely studied (e.g. Pakkanen, 2011; Barndorff-Nielsen et al., 2011, 2013; Corcuera et al., 2013; Bennedsen et al., 2015) and applied to a number of empirical applications (e.g. Veraart and Veraart, 2014; Bennedsen, 2015).

The driftless $\mathcal{BSS}$ process is defined as

$$X_t = \int_{-\infty}^{t} g(t-s)\sigma_s dW_s, \quad t \geq 0,$$

where g is a square integrable kernel function, σ is a stochastic volatility process which is possibly correlated with the driving Brownian motion W. The next section will present the different specifications we consider for σ.

For simulation of the volatility modulated $\mathcal{BSS}$ process we utilize the hybrid scheme of Bennedsen et al. (2015).

C.1.1 Stochastic volatility regimes

For the stochastic volatility process $\sigma = \{\sigma_t\}_{t\in\mathbb{R}}$, we consider three different specifications: (i) constant volatility, labeled NoSV; (ii) one-factor stochastic volatility, labeled SV1F; and (iii) two-factor stochastic volatility, labeled SV2F. For the NoSV model we take for $t \in \mathbb{R}$,

$$\sigma_t = 1,$$

while we in the SV1F model take, following Barndorff-Nielsen et al. (2008),

$$\begin{aligned}
\sigma_t &= \exp(\beta_0 + \beta_1 \tau_t),\\
d\tau_t &= \xi \tau_t dt + dB_t,\\
\mathbb{E}[dW_t dB_t] &= \rho dt,
\end{aligned}$$

where B is a standard Brownian motion and $\beta_1 = 0.125$, $\xi = -0.025$, $\beta_0 = \frac{\beta_1^2}{2\xi} = -0.3125$ and $\rho = -0.3$. Lastly, for the SV2F model we take, following Huang and Tauchen (2005) and Barndorff-Nielsen et al. (2008),

$$\begin{aligned}
\sigma_t &= s\text{-}\exp(\beta_0 + \beta_1 \tau_{1t} + \beta_2 \tau_{2t}),\\
d\tau_{1t} &= \xi_1 \tau_{1t} dt + dB_{1t},\\
d\tau_{2t} &= \xi_2 \tau_{2t} dt + (1 + \phi \tau_{2t}) dB_{2t},\\
\mathbb{E}[dW_t dB_{1t}] &= \rho_1 dt,\\
\mathbb{E}[dW_t dB_{2t}] &= \rho_2 dt,
\end{aligned}$$

where B_1, B_2 are standard Brownian motions and the function $s\text{-}\exp$ is given by

$$s\text{-}\exp(x) = \begin{cases} \exp(x), & x \leq \log(1.5),\\ \frac{3}{2}\sqrt{1 - \log(1.5) + x^2/\log(1.5)}, & x > \log(1.5), \end{cases}$$

and the parameters are set to $(\beta_0, \beta_1, \beta_2)^T = (-1.20, 0.040, 1.50)^T$, $(\xi_1, \xi_2)^T = (-0.00137, -1.386)^T$, $\phi = 0.250$, and $\rho_1 = \rho_2 = -0.30$.

We note that in the NoSV case the process X is Gaussian and can thus be simulated exactly using a Cholesky decomposition of its variance-covariance matrix, which is what we do in our simulations. The stochastic processes of SV1F and SV2F can be simulated exactly using methods in Glasserman (2003), see also the Simulation Appendix to Barndorff-Nielsen et al. (2008).

C.2 Fractional Brownian motion

The fractional Brownian motion (fBm, Mandelbrot and Van Ness, 1968) is the most well-known fractal process. It is the zero-mean Gaussian process B^H, starting at zero, with covariance function

$$Cov(B_t^H, B_s^H) = \frac{1}{2}\left(|t|^{2H} + |s|^{2H} - |t-s|^{2H}\right), \quad t, s \geq 0,$$

where $H \in (0,1)$ is the *Hurst index*. The fBm is self-similar, in the sense that $B^H(at) \overset{d}{=} |a|^H B^H(t)$, where "$\overset{d}{=}$" means equality in distribution. As mentioned in the introduction, this self-similarity implies a deterministic one-to-one relationship between the Hurst index H and the fractal index α (Gneiting and Schlather, 2004). Indeed, we have $H = \alpha + \frac{1}{2}$. What this means is that the small-scale behavior (as governed by α) is determined by the large-scale behavior (as governed by H) and vice versa: when $H < 1/2$ then B^H has rough paths (i.e. $\alpha < 0$) and short memory, while $H > 1/2$ implies that B^H has smooth paths (i.e. $\alpha > 0$) and long memory (in the sense of a non-integrable autocorrelation function). When $H = 1/2$ B^H is a Brownian motion.

The increments of fBm are stationary, and the increment process $X_t^H := B_{t+1}^H - B_t^H$ is called *fractional Gaussian noise* (fGn). The correlation function of the fGn was given in (3.5).

C.3 Cauchy process

The Cauchy process (Gneiting and Schlather, 2004) X is the zero-mean, unit variance, stationary Gaussian process with correlation function

$$\rho(h) = \left(1 + |h|^{2\alpha+1}\right)^{-\frac{\beta}{2\alpha+1}}, \quad h \in \mathbb{R}, \tag{C.1}$$

with $\alpha \in (-1/2, 1/2)$ and $\beta > 0$. See e.g. Gneiting (2000) for arguments showing that these parameter restrictions are necessary and sufficient conditions for (C.1) to be the autocorrelation function of a stationary Gaussian process.

The Cauchy process satisfies the assumptions (A1)–(A3) as shown in Barndorff-Nielsen et al. (2009), Example 3.

C.4 Powered exponential process

The powered exponential process X is the zero-mean, unit variance, stationary Gaussian process with correlation function

$$\rho(h) = \exp\left(-|ch|^{2\alpha+1}\right), \quad h \in \mathbb{R},$$

with $\alpha \in (-1/2, 1/2)$ and $c > 0$. Let us verify that the powered exponential process satisfies assumptions (A1)–(A3). To check (A1), let $x \geq 0$ and write

$$\gamma_2(x) = 2\left(1 - \rho(x)\right) = x^{2\alpha+1} L(x),$$

where

$$L(x) = 2\frac{1-\rho(x)}{x^{2\alpha+1}} = 2\frac{1-\exp\left(-|cx|^{2\alpha+1}\right)}{x^{2\alpha+1}}.$$

Using the rule of L'Hôpital it is easy to show that

$$\lim_{x\to 0} L(x) = 2c^{2\alpha+1} > 0,$$

implying that L is slowly varying at zero. To see that (A2) holds, note that we can write

$$\frac{d^2}{dx^2}\gamma_2(x) = x^{2\alpha-1}L_2(x),$$

where

$$L_2(x) = 2c^{2\alpha+1}(2\alpha+1)\rho(x)\left[2\alpha - c^{2\alpha+1}(2\alpha+1)x^{2\alpha+1}\right].$$

Again, it is easy to see that

$$\lim_{x\to 0} L_2(x) = c^{2\alpha+1}4\alpha(2\alpha+1) \in \mathbb{R},$$

so that also L_2 is slowly varying at zero. Lastly, note that

$$L_2'(x) := \frac{d}{dx}L_2(x) = -2c^{4\alpha+2}(2\alpha+1)^2\rho(x)x^{2\alpha}\left[4\alpha+1-c^{2\alpha+1}(2\alpha+1)x^{2\alpha+1}\right],$$

so that, around a neighborhood of $x = 0$ we have $L_2'(x) < 0$ if $\alpha > -1/4$ and $L_2'(x) > 0$ if $\alpha \leq -1/4$. In other words, in a neighborhood of zero, L_2 is either decreasing or increasing. In both cases we can therefore conclude that for all $b \in (0,1)$,

$$\sup_{y\in[x,x^b]}\left|\frac{L_2(y)}{L(x)}\right| \to |4\alpha|(2\alpha+1) < \infty, \quad x \to 0,$$

which shows that (A3) is fulfilled as well.

References

Achard, S. and J. Coeurjolly (2010). Discrete variations of the fractional Brownian motion in the presence of outliers and additive noise. *Statistics Surveys 4*, 117–147.

Barndorff-Nielsen, O. E. (2012). Notes on the gamma kernel. *Thiele Research Reports* (03).

Barndorff-Nielsen, O. E. (2016). Assessing Gamma kernels and BSS/LSS processes. *CREATES Research Paper 2016-09*.

Barndorff-Nielsen, O. E., F. E. Benth, and A. E. D. Veraart (2013). Modelling energy spot prices by volatility modulated Lévy-driven Volterra processes. *Bernoulli 19*(3), 803–845.

Barndorff-Nielsen, O. E., J. M. Corcuera, and M. Podolskij (2009). Power variation for Gaussian processes with stationary increments. *Stochastic processes and their applications 119*(6), 1845–1865.

Barndorff-Nielsen, O. E., J. M. Corcuera, and M. Podolskij (2011). Multipower variation for Brownian semistationary processes. *Bernoulli 17*(4), 1159–1194.

Barndorff-Nielsen, O. E., J. M. Corcuera, and M. Podolskij (2013). Limit theorems for functionals of higher order differences of Brownian semistationary processes. In A. N. Shiryaev, S. R. S. Varadhan, and E. Presman (Eds.), *Prokhorov and Contemporary Probability Theory*, pp. 69–96. Berlin: Springer.

Barndorff-Nielsen, O. E., P. R. Hansen, A. Lunde, and N. Shephard (2008). Designing realized kernels to measure the ex post variation of equity prices in the presence of noise. *Econometrica 76*(8), 1481–1536.

Barndorff-Nielsen, O. E., P. R. Hansen, A. Lunde, and N. Shephard (2009). Realized kernels in practice: trades and quotes. *The Econometrics Journal 12*, C1–C32.

Barndorff-Nielsen, O. E. and J. Schmiegel (2007). Ambit processes: with applications to turbulence and tumour growth. In *Stochastic analysis and applications*, Volume 2 of *Abel Symp.*, pp. 93–124. Berlin: Springer.

Barndorff-Nielsen, O. E. and J. Schmiegel (2009). Brownian semistationary processes and volatility/intermittency. In *Advanced financial modelling*, Volume 8 of *Radon Series on Computational and Applied Mathematics*, pp. 1–25. Berlin: Walter de Gruyter.

Bayer, C., K. Friz, and J. Gatheral (2015). Pricing under rough volatility. *Working paper available at SSRN: http://ssrn.com/abstract=2554754*.

Bennedsen, M. (2015). Rough electricity: a new fractal multi-factor model of electricity spot prices. *CREATES Research Paper 2015-42*.

Bennedsen, M., U. Hounyo, A. Lunde, and M. S. Pakkanen (2016). The Local Fractional Bootstrap. *Working paper*.

Bennedsen, M., A. Lunde, and M. S. Pakkanen (2015). Hybrid scheme for Brownian semistationary processes. *CREATES Research Paper 2015-43*.

Bennedsen, M., A. Lunde, and M. S. Pakkanen (2016). Decoupling the short- and long-term behavior of stochastic volatility. *Working paper*.

Bingham, N. H., C. M. Goldie, and J. L. Teugels (1989). *Regular Variation*. Cambridge University Press.

Breuer, P. and P. Major (1983). Central limit theorems for nonlinear functionals of Gaussian fields. *Journal of Multivariate Analysis 13*(3), 425–441.

Chan, G. and A. T. A. Wood (2004). Estimation of fractal dimension for a class of non-Gaussian stationary proceses and fields. *Annals of Statistics 32*, 1222–1260.

Coeurjolly, J. (2001). Estimating the parameters of a fractional Brownian motion by discrete variations of its sample paths. *Statistical Inference for Stochastic Processes 4*, 199–227.

Coeurjolly, J. (2008). Hurst exponent estimation of locally self-similar Gaussian processes using sample quantiles. *The Annals of Statistics 36*(3), 1404–1434.

Comte, F. and E. Renault (1996). Long memory continuous time models. *Journal of Econometrics 73*, 101–149.

Comte, F. and E. Renault (1998). Long memory in continuous-time stochastic volatility models. *Mathematical Finance 8*(4), 291–323.

Constantine, A. G. and P. Hall (1994). Characterizing surface smoothness via estimation of effective fractal dimension. *Journal of the Royal Statistical Society: Series B 56*(1), 97–113.

Corcuera, J. M., E. Hedevang, M. S. Pakkanen, and M. Podolskij (2013). Asymptotic theory for Brownian semistationary processes with application to turbulence. *Stochastic processes and their applications 123*(7), 2552–2574.

Davidson, R. and J. G. MacKinnon (1999). The size distortion of bootstrap tests. *Econometric Theory 15*, 361–376.

Davies, S. and P. Hall (1999). Fractal analysis of surface roughness by using spatial data. *Journal of the Royal Statistical Society: Series B 61*, 3–37.

Delbaen, F. and W. Schachermayer (1994). A general version of the fundamental theorem of asset pricing. *Mathematische Annalen 300*, 463–520.

Falconer, K. (1990). *Fractal Geometry: Mathematical Foundations and Applications.* Wiley, Chichester.

Gatheral, J., T. Jaisson, and M. Rosenbaum (2014). Volatility is rough. *Working paper*.

Glasserman, P. (2003). *Monte Carlo Methods in Financial Engineering.* New York: Springer.

Gneiting, T. (2000). Power-law correlations, related models for long-range dependence, and their simulation. *Journal of Applied Probability 37*, 1104–1109.

Gneiting, T. and M. Schlather (2004). Stochastic models that separate fractal dimension and the Hurst effect. *SIAM review 46*(2), 269–282.

Gneiting, T., H. Sevcikova, and D. B. Percival (2012). Estimators of Fractal Dimension: Assessing the Roughness of Time Series and Spatial Data. *Statistical Science 27*(2), 247–277.

Grau-Carles, P. (2005). Tests of long memory: A bootstrap approach. *Computational Economics* (25), 103–113.

Hall, P., W. Härdle, T. Kleinow, and P. Schmidt (2000). Semiparametric bootstrap approach to hypothesis tests and confidence intervals for the Hurst coefficient. *Statistical Inference for Stochastic Processes* (3), 263–276.

Handcock, M. S. and M. L. Stein (1993). A Bayesian analysis of kriging. *Technometrics 35*(4), 403–410.

Huang, X. and G. Tauchen (2005). The relative contribution of jumps to total price variation. *Journal of Financial Econometrics 3*, 456–499.

Kim, Y. M. and D. J. Nordman (2013). A frequency domain bootstrap for Whittle estimation under long-range dependence. *Journal of Multivariate Analysis 115*, 405–420.

Kolmogorov, A. N. (1941). The local structure of turbulence in incompressible viscous fluid for very large Reynolds numbers. *Doklady Akademii Nauk SSSR 30*(4), 299–303.

Mandelbrot, B. B. and J. W. Van Ness (1968). Fractional Brownian motions, fractional noises and applications. *SIAM Review 10*, 422–437.

Matérn, B. (1960). Spatial variation: Stochastic models and their application to some problems in forest surveys and other sampling investigations. *Meddelanden från Statens Skogsforskningsinstitut 49*(5).

Norvaiša, R. (2006). Rough functions: p-variation, calculus, and index estimation. *Lithuanian Mathematical Journal 46*(1), 102–128.

Pakkanen, M. S. (2011). Brownian semistationary processes and conditional full support. *International Journal of Theoretical and Applied Finance 14*(4), 579–586.

Rényi, A. (1963). On stable sequences of events. *Sankhya Ser. A 25*, 293–302.

Shephard, N. (2005). *Stochastic Volatility, Selected Readings.* Oxford University Press.

Taqqu, M. (1975). Weak convergence to fractional Brownian motion and to the Rosenblatt process. *Z. Wahrsch. Verw. Gebiete 31*, 287–302.

Taqqu, M. (1979). Convergence of integrated processes of arbitrary Hermite rank. *Z. Wahrsch. Verw. Gebiete 50*(1), 53–83.

Veraart, A. E. D. and L. A. M. Veraart (2014). Modelling electricity day-ahead prices by multivariate Lévy semistationary processes. In F. E. Benth, V. A. Kholodnyi, and P. Laurence (Eds.), *Quantitative Energy Finance*, pp. 157–188. New York: Springer.

Research Papers 2016

CREATES
Center for Research in Econometric Analysis of Time Series

2016-04: Markku Lanne and Jani Luoto: Data-Driven Inference on Sign Restrictions in Bayesian Structural Vector Autoregression

2016-05: Yunus Emre Ergemen: Generalized Efficient Inference on Factor Models with Long-Range Dependence

2016-06: Girum D. Abate and Luc Anselin: House price fluctuations and the business cycle dynamics

2016-07: Gustavo Fruet Dias, Cristina M. Scherrer and Fotis Papailias: Volatility Discovery

2016-08 N. Haldrup, O. Knapik and T. Proietti: A generalized exponential time series regression model for electricity prices

2016-09: Ole E. Barndorff-Nielsen: Assessing Gamma kernels and BSS/LSS processes

2016-10: Tim Bollerslev, Andrew J. Patton and Rogier Quaedvlieg: Modeling and Forecasting (Un)Reliable Realized Covariances for More Reliable Financial Decisions

2016-11: Tom Engsted and Thomas Q. Pedersen: The predictive power of dividend yields for future inflation: Money illusion or rational causes?

2016-12: Federico A. Bugni, Mehmet Caner, Anders Bredahl Kock and Soumendra Lahiri: Inference in partially identified models with many moment inequalities using Lasso

2016-13: Mikko S. Pakkanen and Jani Lukkarinen: Arbitrage without borrowing or short selling?

2016-14: Andrew J.G. Cairns, Malene Kallestrup-Lamb, Carsten P.T. Rosenskjold, David Blake and Kevin Dowd: Modelling Socio-Economic Differences in the Mortality of Danish Males Using a New Affluence Index

2016-15: Mikkel Bennedsen, Ulrich Hounyo, Asger Lunde and Mikko S. Pakkanen: The Local Fractional Bootstrap

2016-16: Martin M. Andreasen and Kasper Jørgensen: Explaining Asset Prices with Low Risk Aversion and Low Intertemporal Substitution

2016-17: Robinson Kruse, Christian Leschinski and Michael Will: Comparing Predictive Accuracy under Long Memory - With an Application to Volatility Forecasting

2016-18: Søren Johansen and Bent Nielsen: Tightness of M-estimators for multiple linear regression in time series

2016-19: Tim Bollerslev, Jia Li and Yuan Xue: Volume, Volatility and Public News Announcements

2016-20: Andrea Barletta, Paolo Santucci de Magistris and Francesco Violante: Retrieving Risk-Neutral Densities Embedded in VIX Options: a Non-Structural Approach

2016-21: Mikkel Bennedsen: Semiparametric inference on the fractal index of Gaussian and conditionally Gaussian time series data